

INSTITUTE FOR SPACE STUDIES

N. 5
NIS-EP
NIS-ALT
NASA-TM
7N-91-TM
277406
P. 152

TEMPERATURE AND COMPOSITION OF THE MARTIAN ATMOSPHERE

Richard Willis Stewart

(NASA-TM-102905) TEMPERATURE AND
COMPOSITION OF THE MARTIAN ATMOSPHERE
(NASA) 152 p

N90-70763

Unclas
00/91 0277406

GODDARD SPACE FLIGHT CENTER
NATIONAL AERONAUTICS AND SPACE ADMINISTRATION

TEMPERATURE AND COMPOSITION
OF THE
MARTIAN ATMOSPHERE

Richard Willis Stewart

Institute for Space Studies
Goddard Space Flight Center
National Aeronautics and Space Administration

and

Columbia University

ABSTRACT

Calculations have been carried through to determine the thermal structure of the Martian atmosphere. The primary input to these calculations is provided by the following information revealed by the radio occultation experiment aboard the Mariner IV spacecraft:

1. A surface pressure of 5 ± 1 mb.
2. A scale height near the surface of 9 ± 1 km.

and by

3. Solar flux and photoionization cross section data.

Ground-based observations and laboratory experiments indicate a total Mars CO_2 content of 90 ± 27 m-atm and an upper limit of 70 cm-atm for O_2 . We assume: a composition of 80% CO_2 and 20% N_2 at the ground; a surface temperature of 180°K , representing the temperature at the latitude of the Mariner observation; and a mean molecular mass of 40. These values are consistent with the Mariner scale height.

The above data determine the gross properties of the lower atmosphere.

The temperature above the mesopause is computed from the second order form of the thermal conduction equation. Radiative losses by atomic oxygen, carbon monoxide and carbon dioxide are included, and the variation of thermal conductivity with composition is allowed for.

The principal result of the study is the temperature of the Martian exosphere as a function of the solar heating flux. This result is used to obtain the variation of the exospheric temperature over a sunspot cycle. The exospheric temperature is found to vary from 180°K at sunspot minimum to 550°K at sunspot maximum.

A study of the relative effectiveness of CO and O as radiators in the planetary thermosphere is carried out. The results of this study are independent of the atmospheric model and serve as a useful check on numerical studies. In the present model it is found that radiative cooling by O dominates at sunspot minimum and cooling by CO dominates near sunspot maximum.

CONTENTS

	Page
ABSTRACT	ii
LIST OF TABLES	v
LIST OF ILLUSTRATIONS	vi
INTRODUCTION	1
Formulation of the Problem	
Assumption of a lower boundary	
Iterative procedure	
Form of equation	
Solar EUV flux	
Photoionization cross sections	
Heating efficiency	
Conditions on Mars during Mariner encounter	
Radiative cooling	
Summary of Results	
Fig. 1. Ratio of O to CO radiated flux	
2. Variation of Martian exospheric temperature with effective solar EUV flux	
3. Variation of exospheric temperature with solar sunspot cycle	
ATMOSPHERIC COMPOSITION	15
DETERMINATION OF THERMOSPHERIC TEMPERATURE	27
Conduction Equation	
General Considerations on Radiative Cooling	
Rotational Cooling by CO	
Cooling via a Ground State Transition in O	
Vibrational Cooling by CO and CO ₂	
Optical Depth	
Comparison of Total Flux Radiated by CO and O	
Thermospheric Heating	
Heating Function Used in Present Calculation	
Integration of the Thermal Conduction Equation	
THE IONOSPHERE	76
APPENDIX A: DIFFUSION THEORY	89
APPENDIX B: VIBRATIONAL EXCITATION	111
ACKNOWLEDGEMENTS	140
REFERENCES	142

LIST OF TABLES

Table	Page
1. Monthly Averages of Solar 10.7 cm Flux	8
2. Flux and Cross Section Data	60
3. Thermal Conductivities of Species Present in the Martian Thermosphere	68

LIST OF ILLUSTRATIONS

Figure	Page
1. Ratio of O to CO radiated flux	10
2. Variation of Martian exospheric temperature with effective solar EUV flux	12
3. Variation of exospheric temperature with solar sunspot cycle	13
4. Photochemical equilibrium density profiles in the Martian atmosphere	19
5. Comparison of photochemical and diffusion times .	22
6. Comparison of CO and O radiation rates	40
7. Mathematical solutions of the thermal conduction equation	71
B1. Lennard-Jones potential curve	120
B2. Coordinates used in evaluation of the inter- molecular potential	125

INTRODUCTION

Formulation of the Problem

The principal problem treated in this paper is the determination of the thermal structure of the Martian upper atmosphere. The temperature distribution in the upper atmosphere is obtained from integration of the equation of thermal conduction after the heating and cooling terms which enter into this equation are determined.

Assumption of a lower boundary. Conditions in the lower atmosphere of Mars are fairly well known up to an altitude of 50 km through the combination of observations and theoretical studies. From 50 km to the mesopause altitude, the atmospheric structure problem is complicated by the fact that local thermodynamic equilibrium is no longer a valid assumption. For this reason the mesopause altitude and temperature

on Mars have not yet been accurately determined. However, it is very likely that the mesopause altitude lies between 70 and 90 km and the mesopause temperature is about 110° to 130°K . The coupling of the upper atmosphere to the atmosphere below the mesopause is very weak and can be neglected. This suggests a procedure for the investigation of the upper atmosphere in which the mesopause is taken as a starting point for the upward integration of the equation of heat conduction. A similar procedure was used by Jastrow and Kyle (1961) and by Harris and Priester (1962) in studies of the Earth's upper atmosphere. As in the case of the Harris and Priester study, the present model assumes diffusive separation of all components above the lower boundary. By analogy with the properties of the Earth's atmosphere, in which the mesopause altitude is 90 km but diffusive separation sets in only above 110 km, it is probable that on Mars, as on the Earth, atmospheric mixing occurs to a height of some 10 or 20 km above the mesopause. It is not likely that mixing extends any farther than this, because the strong positive temperature gradient of the atmosphere above the mesopause will necessarily suppress vertical mixing on Mars as on the Earth.

In order to check the effect of these assumptions on the major results of the present study, calculations have

been carried out in which (a) the mesopause altitude and temperature are varied within the limits specified above; and (b) the height of the turbopause, i.e., the height to which mixing extends, has been set 10 km above the mesopause altitude. It is found that these variations do not have a significant effect on the thermal structure of the upper atmosphere.

Iterative procedure. The heating and cooling terms depend on the density distributions of the constituents present in the thermosphere and these distributions in turn depend on the temperature. Recourse must thus be made to an iterative method of solution. A zeroeth order temperature profile is assumed and initial density profiles computed therefrom. These densities are then used in the integration of the thermal conduction equation and the improved temperature profile thus obtained used to recompute the densities. This procedure is repeated until successive integrations give nearly the same run of temperatures.

Form of equation. The second order form of the thermal conduction equation has been used in the numerical integrations, as was done by Harris and Priester (1962) in their time-dependent study of the terrestrial thermosphere. This

method offers greater flexibility than integration of first order forms of the equation, since cooling by atomic oxygen may be accurately taken into account and the integration may be started with zero gradient, i.e., at the mesopause. The mass dependence of the thermal conductivity has also been included. It is probably more important to allow for this dependence in studying the Martian atmosphere than it is in terrestrial studies since the principal constituent changes from CO_2 to O in the upper atmosphere of Mars with a correspondingly great variation in thermal conductivity.

Solar EUV flux. The heating of the upper atmosphere results principally from absorption of solar extreme ultraviolet (EUV) flux. The calculation of this heat input to the thermosphere must be regarded as the main uncertainty in obtaining the upper atmosphere temperature distribution. The solar EUV has been measured by Hinteregger et al. (1965) in the wavelength region below 1300\AA . The uncertainties in this data are believed by the experimenters to vary from a factor of 3 to 5 at short wavelengths to $\pm 30\%$ at wavelengths above 250\AA . The longer wavelengths make the most important contribution to the heating; hence the value of $\pm 30\%$ may be taken as a reasonable estimate of the uncertainty of the Hinteregger data for the purposes of this study.

The solar flux data of Hinteregger et al. (1965) have been used as the basis for calculating the heat source. Measured values of the 10.7 cm solar flux over the previous (1954-1965) solar cycle are used to estimate the magnitude of variations in the solar EUV with this cycle as explained below.

Photoionization cross sections. In addition to the uncertainties in the solar flux data, there are differences by a factor of two in published values of photoionization cross sections for some of the constituents present in the Martian thermosphere (Schultz, Holland and Marmo, 1963). The present calculations generally take the average values of published cross section data.

Heating efficiency. Not all the energy contained in the incident solar EUV flux will be available for heating the thermosphere. If an energetic photoelectron excites an optical level of an atmospheric constituent the radiation emitted in the return to the ground state usually is lost from the upper atmosphere. In addition, the products of photodissociation may be left in excited states whose excitation energy is emitted as radiation which will, again, be lost to the upper atmosphere. Finally, the energy lost in the photo-

dissociation of CO_2 may not be recovered in the upper atmosphere; that is, it is likely that the O atoms diffuse to lower altitudes before recombining. The effect of these processes on the efficiency of conversion of solar EUV to upper atmospheric heat has been studied, for the Earth's upper atmosphere, by Walker (1964), and has been discussed by McElroy et al. (1965) in conjunction with a study of the Martian atmosphere. Walker's results indicate an overall heating efficiency of .6 for the Earth's thermosphere. This value is used in the present study of the Martian thermosphere, with an estimated uncertainty of $\pm .1$.

Conditions on Mars during Mariner encounter. The Hinteregger data give an EUV flux in wavelengths below 911\AA of about $3 \text{ ergs/cm}^2\text{sec}$ at the top of the Earth's atmosphere. In July of 1965, when the Mariner fly-by occurred, Mars was at a distance of 1.55 A.U. from the sun, which is somewhat greater than its mean distance of 1.52 A.U. The appropriate flux diminution factor is thus .41, and the flux incident at the top of the Martian atmosphere, corresponding to Hinteregger's measurements, would be $1.2 \text{ ergs/cm}^2\text{sec}$. The day-night average is thus $.60 \text{ erg/cm}^2\text{sec}$ and the average value over the day hemisphere is $.30 \text{ erg/cm}^2\text{sec}$.

It must also be remembered that 1965 was a year of

minimum solar activity and that the Hinteregger data were obtained in July 1963, two years prior to Mariner encounter. Solar EUV flux data for 1965 are not yet available, but Priester (1965) reports that the EUV flux variation with solar cycle can be well correlated with five-month averages of the solar 10.7 cm flux. Accordingly, five-month averages about July 1963 and July 1965 have been computed from the mean monthly values measured by the National Research Council, Ottawa, Canada, and published in Solar-Geophysical Data. The monthly averages for May-September, 1963 and 1965 are given in Table 1. The five-month means are found to be 82.6×10^{-22} watts/m²cps for 1963 and 76.1×10^{-22} watts/m²cps for 1965. It is thus felt that a good working estimate of the flux incident at the top of the Martian atmosphere in the wavelength region below 911⁰Å during July 1965 is .28 erg/cm²sec. This represents a value appropriate to the minimum of the solar cycle. During the previous years of maximum solar activity (1957-1958) the five-month average values of the decimeter flux were near 250×10^{-22} watts/m²cps (Harris and Priester, 1962). An appropriate value for the solar EUV at such times is therefore .92 erg/cm²sec.

Radiative cooling. In contrast to the uncertainties in the magnitude of the EUV heating discussed above, the

Table 1

Monthly Averages of Solar 10.7 cm. Flux

	1963	1965
	(10^{-22} watts/m ² cps)	(10^{-22} watts/m ² cps)
May	87.6	78.1
June	83.5	77.0
July	76.0	74.3
August	80.9	74.8
September	84.9	76.3
Mean	82.6	76.1

effect of radiative cooling by CO_2 , CO, and O can be accurately determined. The relative effectiveness of CO and O as radiators has been investigated independently of the model atmosphere studies. Expressions for the total flux lost from a planetary thermosphere by these constituents have been developed and the effectiveness of each under various conditions of temperature and temperature variation is presented. The results of this study can be used as a check on the numerical models obtained.

Summary of Results

It has been found that the most important thermospheric cooling mechanism is the ground state transition $\text{O}(^3\text{P}_1) \rightarrow \text{O}(^3\text{P}_2)$ in atomic oxygen when the temperature of the exosphere is $\lesssim 300^\circ\text{K}$. For higher temperatures the strong temperature dependence of the flux radiated by CO causes it to become a more effective radiator. Analytic expressions have been developed for the total flux radiated by atomic oxygen and by carbon monoxide. Figure 1 shows the ratio of flux radiated by O to that radiated by CO as a function of the temperature of the radiating zone. The curves are labelled according to values of the scale height gradient.

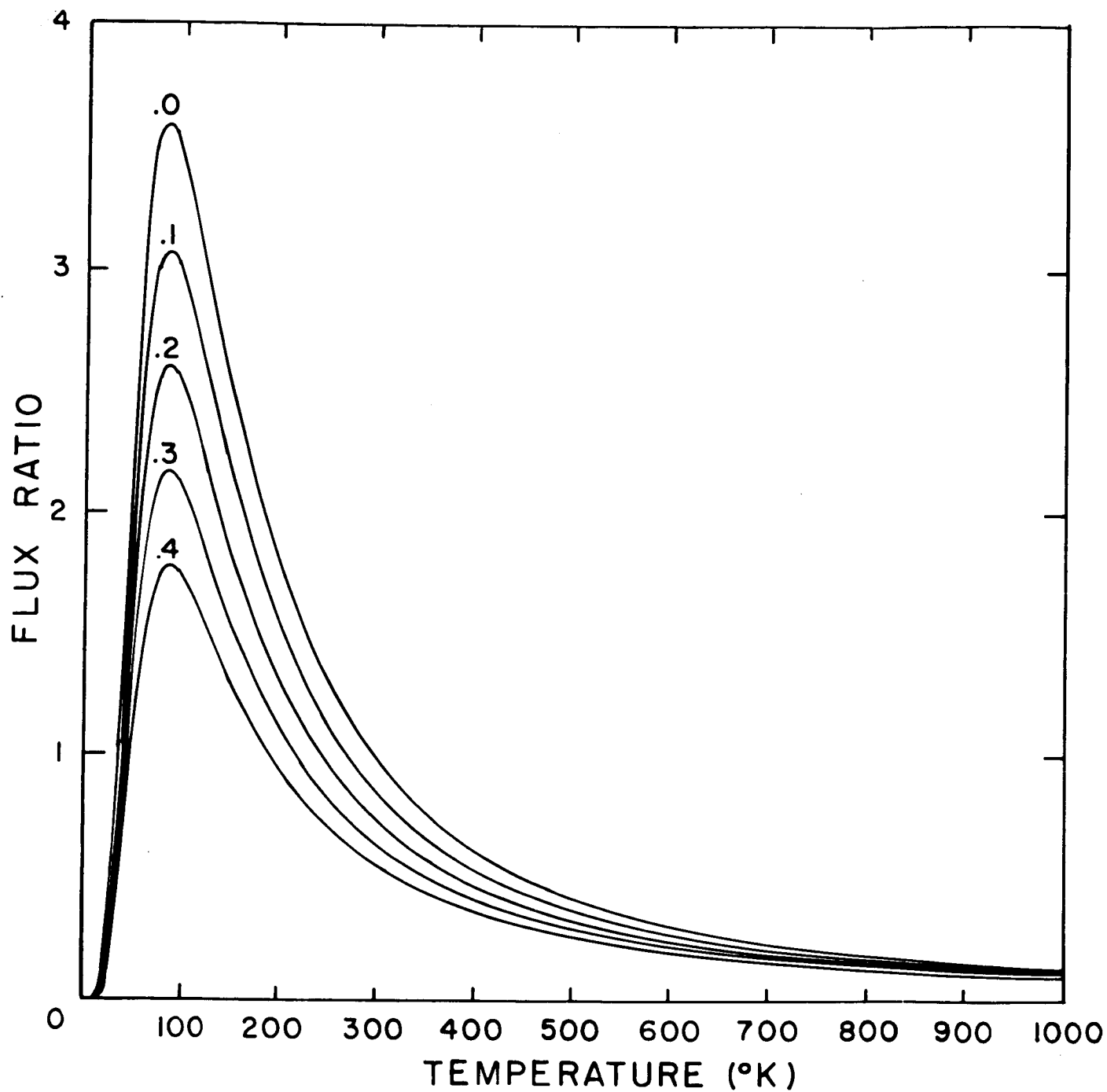


Fig. 1. Ratio of O to CO radiated flux. The curves are labelled according to the value of the scale height gradient (assumed constant).

It has been assumed that the scale height varies linearly in the radiative zone. This analytic study substantiates the results of the numerical computations that a transition occurs near 300°K from a temperature regime in which CO is the principal radiator to one in which O becomes dominant.

The temperature of the Martian exosphere has been found to vary from about 180°K to 550°K depending on the magnitude of the heat input. The lowest temperature values obtained correspond to an effective heating flux of $.14 \text{ erg/cm}^2\text{sec}$ and the highest values to $.55 \text{ erg/cm}^2\text{sec}$, as shown in Fig. 2. This range of EUV flux values corresponds to the probable variation during the 11-year solar cycle, and the range of temperatures therefore represents the low and high values over this period. This is shown in Fig. 3, which gives the variation of the exospheric temperature for the Earth and for Mars as a function of the solar cycle. At the temperature of 550°K , corresponding to the maximum of the sunspot cycle, helium is lost from Mars in a time short compared to the age of the solar system; however, atomic oxygen and neon are retained at this temperature.

The temperature values corresponding to low solar heating flux are consistent with the Mariner IV observations provided the ionosphere is an F_1 layer in which molecular ions (O_2^+) dominate. It has been shown that general consi-

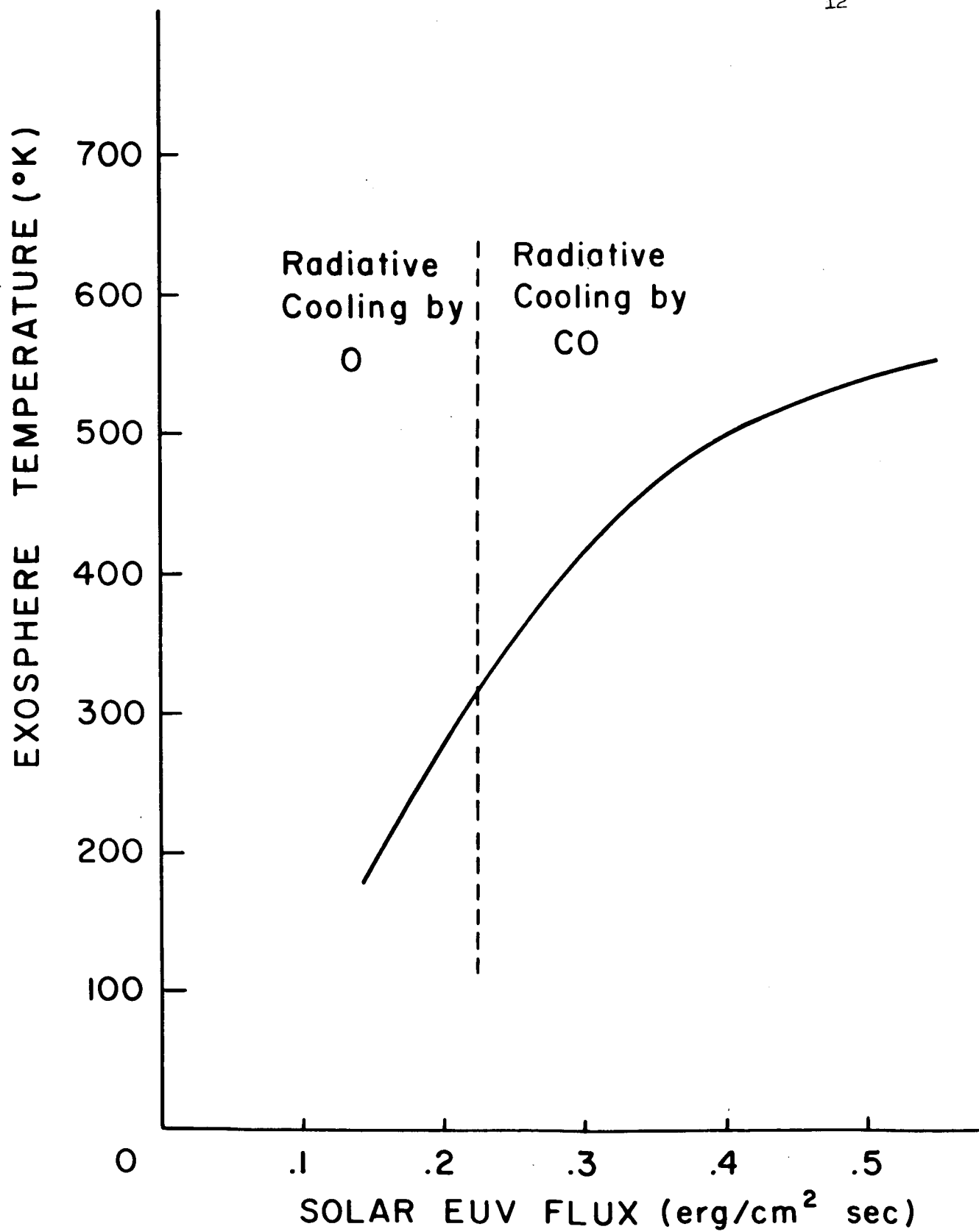


Fig. 2. Variation of Martian exospheric temperature with effective solar EUV flux.

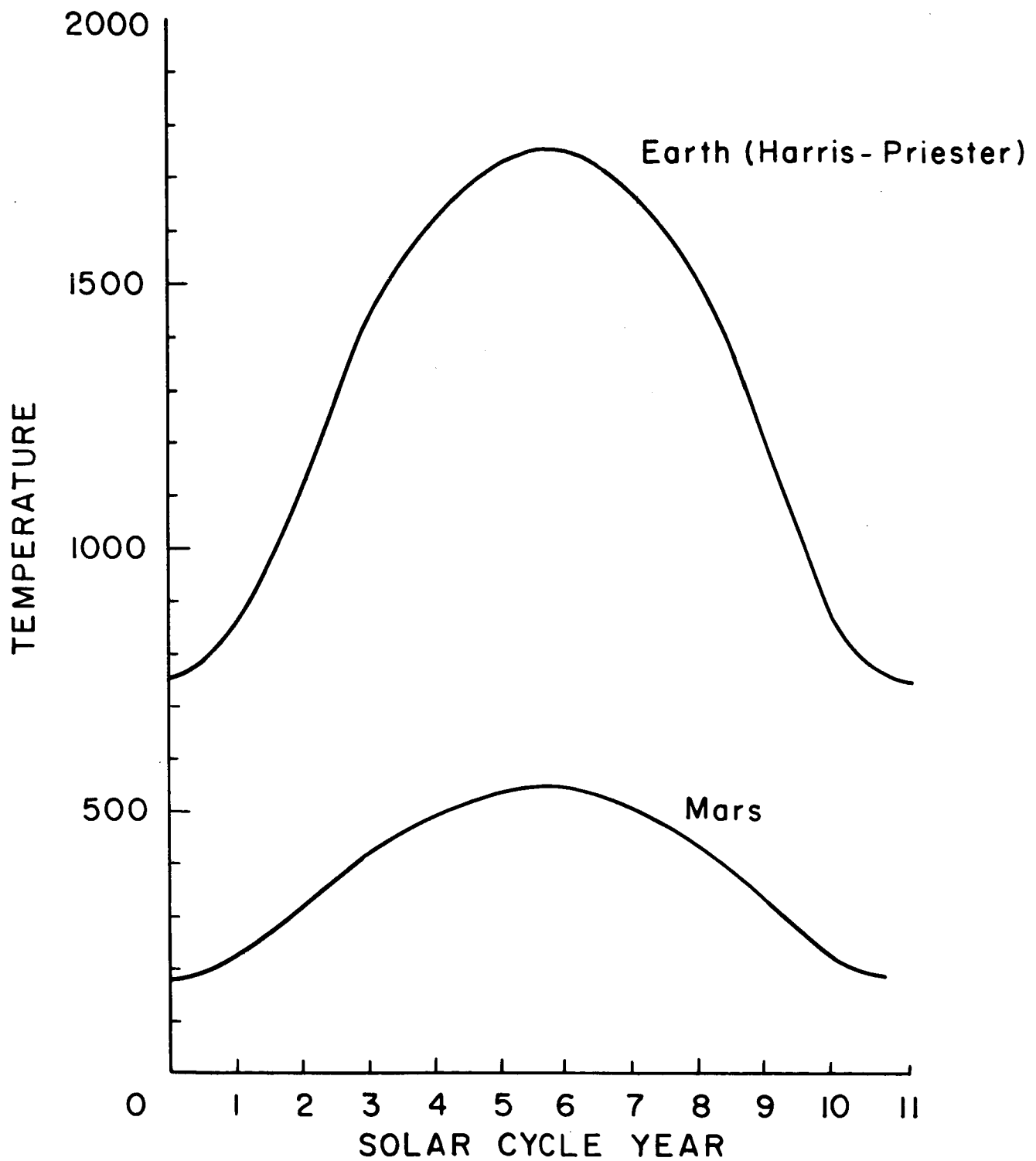


Fig. 3. Variation of exospheric temperature with solar sunspot cycle.

derations of electron production and loss, combined with observational evidence on the slight degree of CO_2 dissociation in the Martian atmosphere lead to the conclusion that the ionosphere is an F_1 layer. It is to be expected that a low heating flux will lead to agreement between the calculated and observed values, since the Mariner IV observations were made at a time of minimum solar activity.

The methods developed in this discussion are applicable to other planetary atmospheres. In each situation the relative importance of the various heating and cooling mechanisms must be studied. The importance of atomic oxygen cooling in the Martian atmosphere is a consequence of the low solar flux values. This cooling mechanism is not temperature sensitive, however, i.e., atomic oxygen cannot act as a thermostat as can carbon monoxide; therefore, in an atmosphere in which CO is absent and O is present, an increase in heating flux will result in much higher temperatures. This is the case on the Earth. Venus possesses an abundance of CO_2 ; moreover, its distance to the sun is half that of Mars, and therefore it receives four times the intensity of solar EUV. These circumstances make it likely that radiative cooling by CO is the dominant cooling process in the atmosphere of Venus.

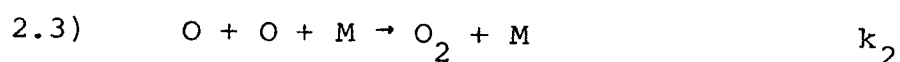
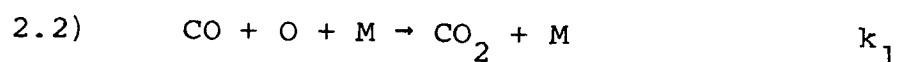
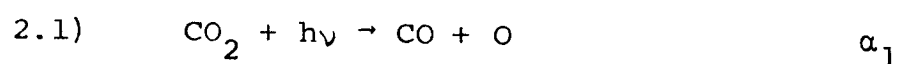
ATMOSPHERIC COMPOSITION

Most estimates of the distribution of constituents in the Martian atmosphere have been based to some extent on the assumption of photochemical equilibrium between products arising in the photodissociation of CO_2 . The following sections will review briefly the photochemical theory and investigate its validity. The role played by diffusion in the Martian atmosphere will be discussed from a qualitative viewpoint in this section. A formal study of the diffusion equations is carried out in Appendix A.

The current theory of photochemical equilibrium and related physical arguments lead to conclusions in direct contradiction to observations of the Martian atmosphere. Recent experimental work (Hartek et al., 1966) suggests a qualitative resolution of this problem. With the present state of affairs the density distributions must therefore be taken as parameters of the overall problem of atmospheric composition,

and temperature studies must be carried out using a variety of feasible compositions.

CO_2 is dissociated by solar ultraviolet radiation in the wavelength interval $1100\text{\AA} - 1800\text{\AA}$. The photochemistry of CO_2 has been investigated by Marmo and Warneck (1961), and by Shimizu (1963), who apply their results to the atmospheres of Mars and Venus respectively. The photodissociation of CO_2 and recombination of the products CO and O are described by the following set of reactions:



In these reactions M represents any third body, the k 's are the three-body rate coefficients, and the α 's are the photodissociative production rates. The rate coefficients are $k_1 = 1.4 \times 10^{-34} \text{ cm}^6/\text{sec.}$ and $k_2 = 2.7 \times 10^{-33} \text{ cm}^6/\text{sec.}$ (Barth, 1964), and the α 's can be computed from

$$2.5) \quad \alpha_i(z) = \int_{\lambda_1}^{\lambda_2} d\lambda \sigma_i(\lambda) F_\infty(\lambda) e^{-\frac{1}{\mu} \sum_j \sigma_j(\lambda) \int_z^\infty n_j(z') dz'}$$

$\sigma_i(\lambda)$ is the photodissociation cross section for the i^{th} molecular species, $F_\infty(\lambda)$ the flux incident at the top of the atmosphere, and μ the cosine of the solar zenith angle. The sum over j accounts for absorption by all the constituents which absorb in the wavelength interval $\lambda_1 - \lambda_2$, and $n_j(z)$ is the number density of the j^{th} absorbing species. In practice the integral over wavelength is replaced by a sum over discrete wavelength intervals.

From the set of equations 2.1 - 2.4 we can derive the equilibrium CO/CO₂ ratio and find

$$2.6) \quad \frac{n_{\text{CO}}}{n_{\text{CO}_2}} = \frac{R}{n_{\text{CO}_2}^{(0)} - R},$$

where $n_{\text{CO}_2}^{(0)}$ is the density of CO₂ available for dissociation and

$$2.7) \quad R = \frac{\alpha_1(z)}{2k_1 n_M(z)} \left[\sqrt{1 + 4k_1 \frac{n_M n_{\text{CO}_2}^{(0)}}{\alpha_1(z)}} - 1 \right].$$

This ratio is height-dependent. At high altitudes 2.6 shows $n_{\text{CO}}/n_{\text{CO}_2} \rightarrow \infty$, indicating complete photodissociation of CO₂.

At the height of the CO maximum, obtained from a complete solution of 2.1 - 2.4, it can be shown that $n_{\text{CO}}/n_{\text{CO}_2} \approx 4$, and CO_2 is substantially dissociated at this level. The high degree of dissociation of CO_2 is a direct consequence of the stability of the CO molecule against oxidation, as reflected in the small value of the rate coefficient k_1 of 2.2.

We will tentatively accept equations 2.1 - 2.4 as an accurate description of the Martian photochemistry in order to discuss the role that diffusion might play in this case.

A solution of the equilibrium rate equations arising from 2.1 - 2.4 shows that CO_2 is dissociated between 70-90 km. on Mars, that there is a sharply peaked O_2 profile in this region and that at higher altitudes CO and O fall off with the scale height of CO_2 (Fig. 4).

The slope with which these density profiles change nowhere corresponds to a fall-off according to their own scale heights, and there is therefore a possibility that they might be unstable. Thus, although solution of the photochemical equations might constitute a first step in the determination of atmospheric composition, their value as accurate representations of the actual density profiles is questionable. The basic reason for this is that the time required for processes such as mixing and diffusion to redistribute the various

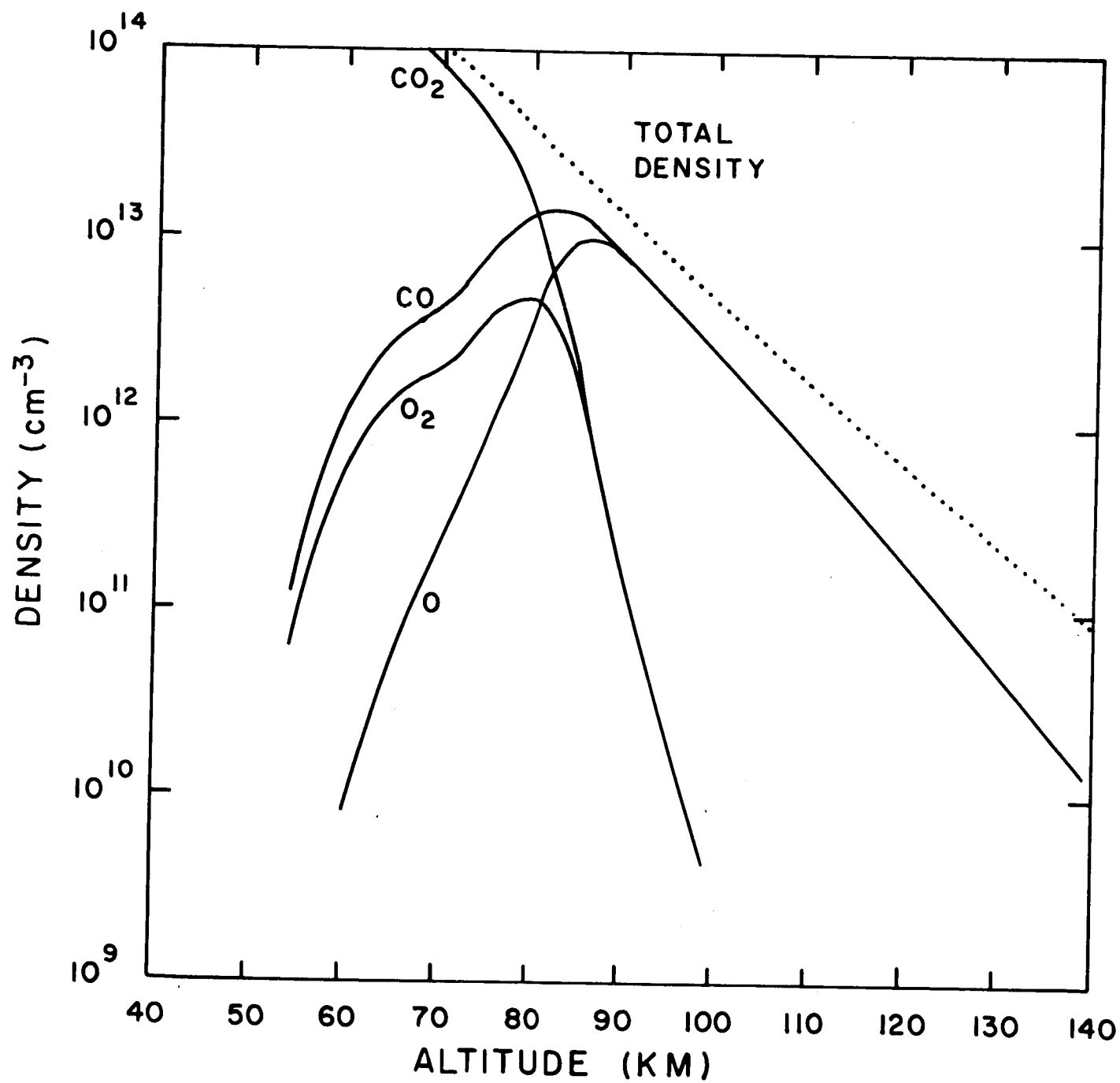


Fig. 4. Photochemical equilibrium density profiles in the Martian atmosphere.

constituents may be short relative to the time required for a complete photochemical cycle, so that, e.g., a CO molecule which is photochemically created at one height in the atmosphere may be transported to another height before being oxidized. The true density distributions are thus the result of several physical processes the relative importance of which can be investigated by comparing their characteristic lifetimes.

The photochemical lifetime of a constituent may be defined as the time which a molecule or atom could be expected to spend in the atmosphere before suffering a chemical reaction which removes it. If L denotes the loss rate of a constituent and n its number density, the photochemical lifetime may be defined by

$$2.8) \quad \tau_p = \frac{n}{L} \quad .$$

The loss rates can be determined from the rate equations for the reactions 2.1 - 2.4. For example, the rate equation for CO is

$$2.9) \quad \frac{dn_{CO}}{dt} = \alpha_1 n_{CO_2} - k_1 n_M n_O n_{CO} \quad ,$$

and the photochemical lifetime is then

$$2.10) \quad \tau_p(\text{CO}) = \frac{n_{\text{CO}}}{k_1 n_{\text{M}} n_{\text{O}} n_{\text{CO}}} = \frac{1}{k_1 n_{\text{M}} n_{\text{O}}} .$$

The diffusion time for a given constituent is defined as the time required for its molecules to diffuse through a distance equal to its own scale height. Thus

$$2.11) \quad \tau_D = \frac{H}{W_D} ,$$

where W_D is the diffusion velocity. It is shown in Appendix A (A.9) that, to close approximation $W_D = D/H$, where D is the diffusion coefficient, hence the diffusion time may be written

$$2.12) \quad \tau_D = \frac{H^2}{D} .$$

The results of comparing the photochemical and diffusive times are shown in Fig. 5. These results show clearly that diffusive effects can be important in determining the density profiles of the various constituents. For example, the curves for CO_2 and CO show that the photochemical lifetime is nearly everywhere greater than the diffusion time, and thus the photochemical density profiles for these constituents are probably greatly in error. It would not be correct to

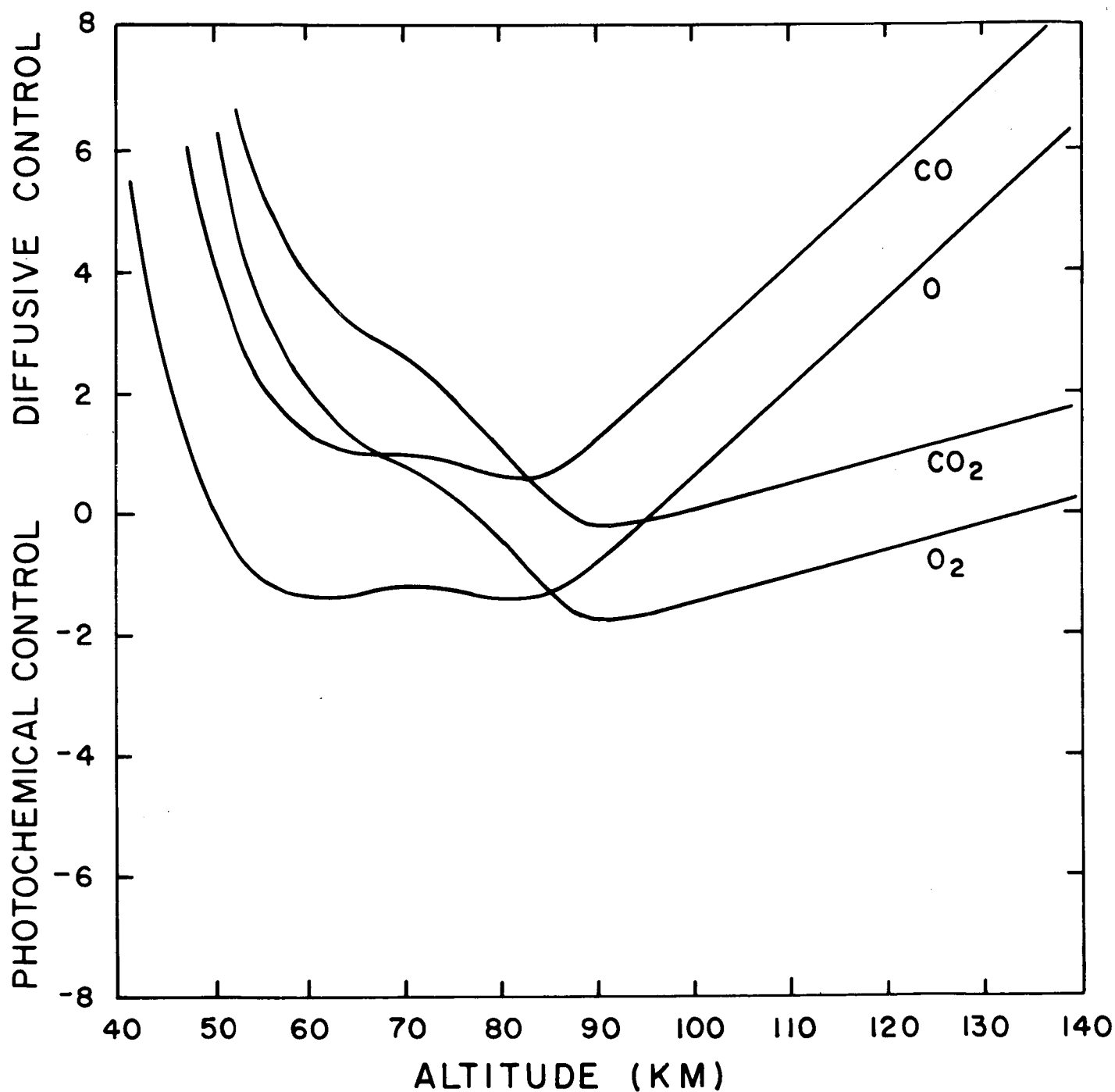


Fig. 5. Comparison of photochemical and diffusion times. The density distributions may be approximated by their photochemical equilibrium values in altitude regions where these curves have negative values.

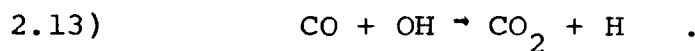
conclude, however, on the basis of these comparisons, that the CO_2 in the upper Martian atmosphere is only slightly dissociated. CO_2 may follow a diffusive profile in the upper atmosphere but still be highly dissociated. The determining factor in this regard is the ease with which the dissociation products CO and O recombine to form CO_2 . If CO is easily oxidized we might expect CO_2 to be slightly dissociated, but, on the other hand, if CO is difficult to oxidize then CO_2 must be highly dissociated. We might, for example, picture a process where a CO_2 molecule at some level in the atmosphere is dissociated. The products CO and O then diffuse downward through about a scale height and recombine to form CO_2 , which is then available to replace, via upward diffusion, that which was dissociated at the higher level. If this picture were qualitatively accurate, CO_2 would be only slightly dissociated. Fig. 5, however, shows that the photochemical lifetime of CO is everywhere greater (by at least a factor of 2.5) than the diffusion time; hence, on the basis of 2.1 - 2.4, the CO_2 in the Martian upper atmosphere would be highly dissociated. The same considerations apply if it is assumed that the constituents are mixed. CO_2 could follow a mixing profile and still be dissociated. The key question is the relative ease with which CO can be oxidized at about one scale height below the altitude of CO_2 .

dissociation. It may be pointed out in this regard that the O_2 in the Earth's atmosphere is found to follow a nearly diffusive profile but that it is nonetheless about 90% dissociated in the upper atmosphere (Nicolet and Mange, 1954). Atomic oxygen is, indeed, the dominant constituent throughout an extensive region of the Earth's atmosphere and it is more easily oxidized than CO. We must thus accept the conclusion that, if CO is as difficult to oxidize as the rate constant of 2.2 implies, CO_2 must be a minor constituent above the dissociation level.

On the basis of 2.1 - 2.4 the dissociation altitude in the Martian atmosphere occurs near 80 km., but further consideration of the effects of diffusion show that it would actually occur at much lower levels. In the absence of any reaction to remove O_2 at low altitudes, there is nothing to prevent its downward diffusion. If substantial downward diffusion occurs, the remaining atomic oxygen would be more readily oxidized to replace the diffusive loss of O_2 . This would hinder the oxidation of CO and, by the same token, enhance the dissociation of CO_2 at the altitude from which diffusive loss of O_2 occurred. Downward diffusion of O_2 will lower the altitude at which dissociation of CO_2 takes place, and this lowering will increase the relative abundance of CO and O at higher levels.

Acceptance of the photochemical equations 2.1 - 2.4 and their rate constants, combined with straightforward arguments concerning the effect of diffusion, thus leads to two conclusions regarding the Martian atmosphere: it must be dissociated down to a lower level than would be found from photochemical calculations alone, and CO_2 can only be a minor constituent above the dissociation level.

These conclusions are not compatible with observation. Dissociation of CO_2 to about one or two scale heights above the ground would leave roughly 50 m-atm. of CO_2 , whereas Owen (1966) and Spinrad et al. (1966) have reported a CO_2 content in excess of this figure. In addition to these spectroscopic results, Harteck et al. (1966) have reported experimental evidence indicating that CO_2 is much less dissociated than would be predicted from the carbon-oxygen photochemistry alone. They attribute this to the possibility of rapid oxidation of CO in the presence of trace amounts of hydrogen compounds, e.g.,



No estimates of reaction rates for such oxidation are given.

The amount of water vapor in the Martian atmosphere is small. Kaplan, Münch and Spinrad (1964) give $14 \pm 7 \mu$, and

Spinrad et al. (1966) in their report on the CO_2 observations mention 10-30 μ for water vapor. This is an overall abundance of $\sim .0002\%$, but since the water vapor scale height is determined by the saturated vapor pressure curve and not by hydrostatic balance, the percentage composition will be much higher near the ground. If the presence of water vapor in the atmosphere is the cause of the rapid oxidation of CO, then the CO formed in photodissociation of CO_2 at high altitudes must have access to water vapor near the ground. It is therefore reasonable to assume that the Martian turbopause must be at least as high as the level at which dissociation of CO_2 occurs, i.e., at or above the 70-90 km. level.

In view of the uncertainties regarding both the reactions which constituents undergo and the effectiveness of mixing and diffusion in redistributing them, it is necessary to regard the atmospheric composition as a parameter to be varied in an effort to obtain temperature and density values compatible with observation. In the study of the thermospheric temperature which follows, this is effected by assuming varying degrees of CO_2 dissociation and varying altitudes at which this dissociation occurs.

DETERMINATION OF THERMOSPHERIC TEMPERATURE

The temperature distribution in the upper atmosphere is a consequence of the processes of energy deposition and loss occurring there and of the relative altitudes at which these processes are effective. The principal source of thermospheric heating is the solar ultraviolet radiation which is deposited via photoionization of the constituents present at high altitudes. The detailed mechanisms by which solar radiation is transformed into heat in the upper atmosphere is not completely understood but a reasonably accurate description of the heating function can be given.

The heat deposited in the thermosphere is lost by means of conduction and radiation. Radiative loss occurs by infrared emission from excited states of constituents present in the thermosphere, and this section will be mainly directed toward deriving the functional forms of these loss terms and studying their effectiveness.

Conduction Equation

The energy balance in the highest regions of a planetary atmosphere is described by the equation of thermal conduction, conduction being the most efficient means of energy transport in these regions. The equation determining the temperature may be written

$$3.1) \quad C_v \rho \frac{\partial T}{\partial t} = \frac{\partial}{\partial z} \left[K(z, T) \frac{\partial T}{\partial z} \right] + Q(z, t; T) \quad ,$$

where C_v is the specific heat at constant volume, ρ the mass density, $K(z, T)$ the thermal conductivity, T the absolute temperature, and Q the net rate of heat generation per unit volume and time. The main problem in solving 3.1 is the determination of the functional form of $Q(z, t; T)$. This form will normally be sufficiently complicated to require numerical integration of the equation. As a first step we write

$$3.2) \quad Q(z, t; T) = q(z, t; T) - L(z, t; T) \quad ,$$

expressing the net rate of heat generation as the difference between heat sources q and sinks L .

General Considerations on Radiative Cooling

Cooling of the upper atmosphere occurs via conduction of the heat deposited there and by radiative loss. The conduction is expressed by the spatial derivatives in 3.1, and the radiative loss is represented by the L of 3.2. Radiative loss of heat occurs when an atom or molecule which has been collisionally excited de-excites via emission of a photon in an optically thin region of the atmosphere. The form of L for a given cooling mechanism depends on whether or not collisions are sufficiently frequent to establish a Boltzman distribution among the energy levels from which cooling may occur. The levels under consideration will be so populated if the rate at which collisional excitation to these levels occurs is much greater than the rate of radiative de-excitation from them. In general terms, if we have a two-level system under consideration, this condition may be written

$$3.3) \quad \eta_c P_{12} n_1 n_M \gg A_{21} n_2 \quad ,$$

where η_c is the collision rate, P_{12} the probability that a collision will result in excitation from level 1 to level 2, A_{21} the Einstein coefficient of spontaneous emission from level 2 to level 1, n_M the total particle density,

and n_1 and n_2 the particle densities in states 1 and 2.

If 3.3 holds, the radiative loss term in 3.2 is relatively easy to determine from general statistical considerations,

but if we have the other extreme, i.e., $\eta_c P_{12} n_1 n_M \ll A_{21} n_2$, the loss rate is determined by the rate of collisional excitation, which must be calculated in each specific case.

Of course, such calculation may be required in any event to determine the validity of 3.3, but often reasonable, though non-rigorous, arguments may be advanced in justification of 3.3 without detailed calculation of the left-hand-side.

The Einstein coefficient may be calculated from the formula (Schiff, 1955, Chapter 15)

$$3.4) \quad A_{21} = \frac{4e^2 \omega_{21}^3}{3\hbar c^3} \left| \langle f | \vec{r} | i \rangle \right|^2 ,$$

where $\langle f | \vec{r} | i \rangle$ is the matrix element of the dipole moment operator between the initial and final states, ω_{21} is the angular frequency of the transition, and the other notation is standard.

If 3.3 holds, the cooling will be said to be emission limited. If the converse is true, the cooling will be said to be collision limited.

In an atmosphere containing the dissociation products of CO_2 , the cooling term is given by

$$3.5) \quad L = R_r(\text{CO}|z, T) + R_s(\text{O}|z, T) + R_v(\text{CO}_2|z, T) \quad .$$

$R_r(\text{CO}|z, T)$ represents emission from the CO rotational levels, $R_s(\text{O}|z, T)$ represents the cooling due to a transition between levels of the ground state term of atomic oxygen $\text{O}(^3P_1) \rightarrow \text{O}(^3P_2)$, and $R_v(\text{CO}_2|z, T)$ represents vibrational transition in CO_2 . A study of vibrational excitation is carried through in Appendix B with reference to the CO molecule. This study indicates that vibrational cooling by CO is negligible.

Rotational Cooling by CO

It is generally true that rotational states are readily populated by collisions (Zener, 1931). A Boltzmann distribution is therefore assumed in what follows, i.e., the radiation is emission limited.

The general expression for the Einstein coefficient for spontaneous emission between adjacent rotational states of a rigid rotator may be written

$$3.6) \quad A_{J, J-1}^{MM'} = \frac{4e^2}{3\hbar} \left[\frac{\omega_{J, J-1}}{c} \right]^3 \left| \langle JM | \vec{r} | J-1 M' \rangle \right|^2 \quad .$$

The matrix element appearing in this expression is most

conveniently evaluated if the dipole moment operator is expressed in terms of the spherical harmonics defined as in Fano and Racah's (1959) (hereafter referred to as F.R.) equation 5.19, i.e., we replace \vec{r} by $\xi \mathcal{C}^{[1]}$, where $e\xi$ is the measured dipole moment of CO. Since \vec{r} and $\mathcal{C}^{[1]}$ are related by a unitary transformation, the square of the matrix element in 3.6 may be written

$$\xi^2 \left| \langle J M | \mathcal{C}^{[1]} | J-1, M' \rangle \right|^2 .$$

The rigid rotator wave functions are the normalized spherical harmonics defined as in F.R. Chapter 5

$$3.7) \quad \psi_{JM} = Y_M^{[J]}(\theta, \varphi) ,$$

and the matrix element to be evaluated is thus

$$3.8) \quad \langle J M | \mathcal{C}_m^{[1]} | J-1, M' \rangle = \int d\Omega Y_M^{[J]*} \mathcal{C}_m^{[1]} Y_{M'}^{[J-1]} .$$

The dependence on the m^{th} component of the dipole moment is included here, and these component contributions will ultimately be summed. The integral in 3.8 has been evaluated by F.R. 14.11 with the result

$$3.9) \quad \langle J M | \mathcal{C}_m^{[1]} | J-1, M' \rangle = i^{2J} (-)^{J-M} \sqrt{(2J+1)(2J-1)} \\ \times (1, J-1, J)_0 \bar{V}_{m M' -M}^{[1 J-1 J]} .$$

The notation $(1, J-1, J)_0$ has been used as a shorthand for $\bar{V} \begin{bmatrix} 1 & J-1 & J \\ 0 & 0 & 0 \end{bmatrix}$, and the \bar{V} coefficients are defined in F.R. Chapter 10. From F.R. 10.16 we have

$$3.10) \quad (abc)_0 = \Delta(a, b, c) \frac{(-1)^g g!}{(g-a)! (g-b)! (g-c)!} ,$$

$$\text{where } \Delta(a, b, c) = \left[\frac{(a+b-c)! (b+c-a)! (c+a-b)!}{(a+b+c+1)!} \right]^{\frac{1}{2}} \text{ and } a+b+c = 2g .$$

Hence

$$3.11) \quad (1, J-1, J)_0 = (-1)^J \left[\frac{J}{(2J-1)(2J+1)} \right]^{\frac{1}{2}} .$$

Using 3.11 and 3.9 we see that the Einstein coefficient for the transition $JM \rightarrow J-1, M'$ caused by the component m of the dipole moment operator is

$$3.12) \quad A_{J, J-1}^{MM'}(m) = \frac{4}{3\hbar} \left[\frac{\omega_{J, J-1}}{c} \right]^3 d^2 J \left\{ \bar{V} \begin{bmatrix} 1 & J-1 & J \\ m & M' & -M \end{bmatrix} \right\}^2 ,$$

where $d = e\xi$ is the dipole moment. The rate of energy loss due to the transition $J \rightarrow J-1$ is

$$3.13) \quad R_J = \sum_{MM'} \sum_{M=-1}^1 A_{J, J-1}^{MM'}(m) N_{JM}(\text{CO}) \hbar \omega_{J, J-1} .$$

The number of molecules occupying the state specified

by J, M is related to the total number in the state J by

$$3.14) \quad N_{JM} = \frac{N_J}{2J + 1} ,$$

since the molecular energy is independent of the magnetic quantum number M . The number of molecules in state J is, in turn, related to the total number density N by

$$3.15) \quad N_J = \frac{Ng_J}{Z_r} e^{-\epsilon_J/kT} ,$$

where Z_r is the rotational partition function, $g_J = 2J + 1$ is the statistical weight of level J , and ϵ_J is the energy of this level. The partition function is

$$3.16) \quad Z_r = \sum_J (2J + 1) e^{-\epsilon_J/kT} .$$

In terms of the rotational constant $B = \hbar/4\pi cI$ of the molecule, the energy of the J^{th} level can be written

$\epsilon_J = hcBJ(J+1)$. If we define a rotational temperature by

$$3.17) \quad \theta_r = \frac{hcB}{k}$$

the partition function becomes

$$3.18) \quad Z_r = \sum_J (2J + 1) e^{-\frac{\theta_r}{T} J(J+1)} .$$

For values of T such that $T \gg \theta_r$ in 3.18 or, equivalently, such that $\epsilon_J \ll kT$ in 3.16, the summation over J may be replaced by an integration over ϵ_J . For CO, $B = 1.93 \text{ cm}^{-1}$ (Bates, 1951) and $\theta_r \approx 3^\circ\text{K}$. Thus, for all but very low temperatures the partition function may be written

$$3.19) \quad Z_r = \int_0^\infty e^{-\epsilon_J/kT} \frac{d\epsilon_J}{hcB} = \frac{kT}{hcB} = \frac{T}{\theta_r} .$$

Using 3.12, 3.13, 3.15, and 3.19, the expression for the cooling rate, 3.13, becomes

$$3.20) \quad R_J = \frac{4}{3} \frac{\theta_r}{T} c d^2 \left[\frac{\omega_{J,J-1}}{c} \right]^4 n_{CO} J e^{-\epsilon_J/kT} \sum_{MM'm} \left\{ \bar{V} \begin{bmatrix} 1 & J-1 & J \\ m & M' & -M \end{bmatrix} \right\}^2 .$$

From F.R. 10.20 the sum over magnetic quantum numbers is just unity, and R_J is given by 3.20 without the summation factor. With $\omega_{J,J-1}/c = 4\pi BJ$ the cooling rate may be written

$$3.21) \quad R_J = \frac{2^{10} \pi^4}{3} \frac{hc}{kT} c d^2 (BJ)^5 e^{-\epsilon_J/kT} n_{CO} .$$

The total rotational cooling rate is the sum of this expression over all J values. Consistent with the approximation made in the evaluation of the partition function, $T \gg 3^\circ\text{K}$, this sum over J may be replaced by an integral. The rotational cooling is thus

$$3.22) \quad R_r(\text{CO}|z) = \frac{2^{10}\pi^4}{3} cd^2 B^4 \left[\frac{\theta_r}{T} \right] n_{\text{CO}} \int_0^\infty J^5 e^{-\frac{\theta_r}{T} J^2} dJ ,$$

which results in

$$3.23) \quad R_r(\text{CO}|z) = \frac{2^{10}\pi^4}{3} cd^2 B^4 n_{\text{CO}} \left[\frac{T}{\theta_r} \right]^2$$

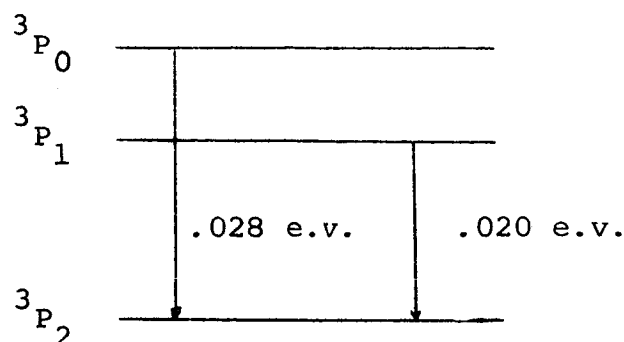
or

$$3.24) \quad R_r(\text{CO}|z) = 2.58 \times 10^{-23} n_{\text{CO}} T^2 ,$$

where we have taken $d = .12 \times 10^{-18}$ (Fowler, 1955).

Cooling via a Ground State Transition in Atomic Oxygen

Cooling via transitions within the ground state triplet of atomic oxygen has been considered by Bates (1951). The possible transitions are schematically indicated below.



The energies ϵ_1 and ϵ_0 of the 3P_1 and 3P_0 levels are, respectively, .020 e.v. and .028 e.v. above the 3P_2 level, and the Einstein coefficients of the indicated transitions are $A_{02} = 1.7 \times 10^{-5} \text{ sec}^{-1}$ and $A_{12} = 8.9 \times 10^{-5} \text{ sec}^{-1}$. Due to the greater excitation energy of the 3P_0 level, the small statistical weight, $g_0 = 1$, and the relative magnitudes of the Einstein coefficients, emission from the 3P_0 state is neglected relative to that from 3P_1 . The condition 3.3 that cooling be emission limited is thus

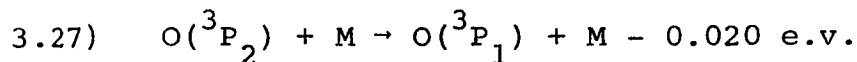
$$3.25) \quad P_{12} \gg \frac{A_{12}}{\eta_c n_M} \frac{g_1}{g_2} e^{-\epsilon_1/kT}.$$

Using $\eta_c \approx 5 \times 10^{-10} \text{ cm}^3/\text{sec}$, as quoted by Bates, and writing the equation in terms of P_{21} rather than P_{12} we

have, with $g_1 = 3$, $g_2 = 5$

$$3.26) \quad P_{21} \gg \frac{1.0 \times 10^5}{n_M} .$$

By citing experimental results on reactions similar to



Bates argues that it is reasonable to assume $P_{21} > 10^{-4}$, and thus that 3.26 should hold up to total densities $\leq 10^9 \text{ cm}^{-3}$.

We will tentatively assume that radiation by atomic oxygen is effective at altitudes below that at which the density is 10^9 .

This point will be re-examined after radiative transfer in the 62μ line is considered. The radiative cooling term for oxygen thus has the form

$$3.28) \quad R_s(O|z, T) = \epsilon_1 A_{12} n(O|{}^3P_1) \\ = \epsilon_1 A_{12} n_O(z) \left[\frac{g_1 e^{-\epsilon_1/kT}}{g_2 + g_1 e^{-\epsilon_1/kT} + g_O e^{-\epsilon_O/kT}} \right]$$

$$3.29) \quad R_s = 2.85 \times 10^{-18} n_O f(T) ,$$

where

$$3.30) \quad f(T) = \frac{g_1 e^{-\epsilon_1/kT}}{g_2 + g_1 e^{-\epsilon_1/kT} + g_0 e^{-\epsilon_0/kT}} .$$

The temperature dependence of 3.29 is not very strong. The factor $f(T)$ varies between 0 and 1/3 for T between 0 and ∞ . The ratio of CO to O radiation rates is seen from 3.24 and 3.29 to be

$$3.31) \quad \frac{R_r}{R_s} = 1.0 \times 10^{-5} \frac{n_{CO}}{n_O} \frac{T^2}{f(T)} .$$

This ratio is shown in Fig. 6 as a function of T for various values of n_{CO}/n_O .

A simple comparison of R_r with R_s as in 3.31 does not necessarily give an accurate description of the relative effectiveness of these constituents in cooling a planetary thermosphere. This is due to the fact that radiation is only effective from about one optical depth and the overlying number densities of CO and O which correspond to unit optical depth are quite different, as will be established below. The comparison is made at this point, however, to indicate the possibility of a range of physical circumstances under which atomic oxygen may be a more effec-

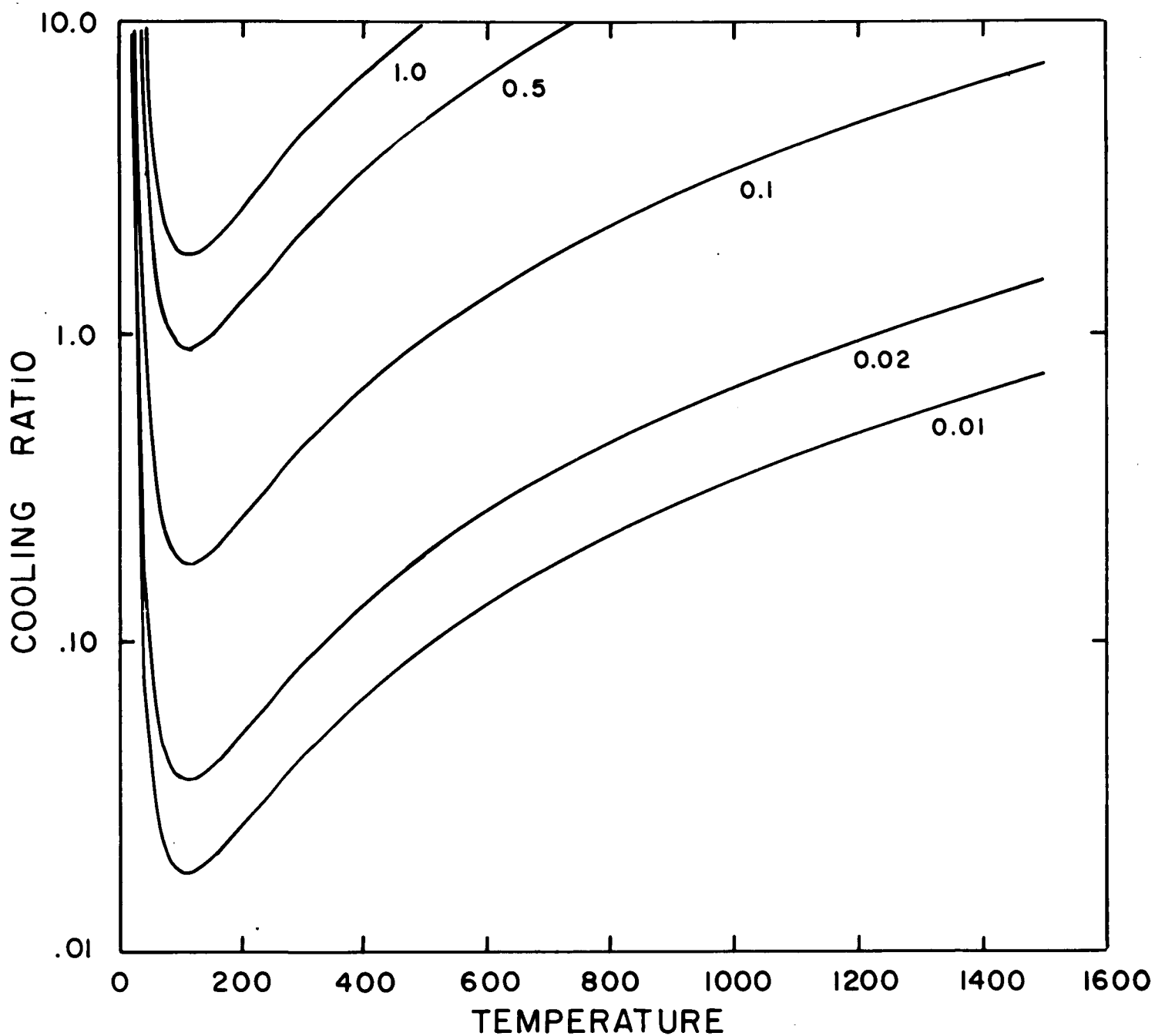


Fig. 6. Comparison of CO and O radiation rates. The curves are labelled according to the assumed n_{CO}/n_O ratio.

tive radiator than carbon monoxide.

Vibrational Cooling by CO and CO₂

The possible importance of CO as a cooling agent in the Martian atmosphere was first pointed out by Chamberlain (1962). In his original paper on the subject he assumed that radiation from the first vibrational state of CO was the principal cooling mechanism and wrote the cooling term as

$$3.32) \quad R_v(\text{CO } z, T) = N^2(z) f(\text{CO}) \eta_{21} h\nu e^{-h\nu/kT} ,$$

where N is the total number density, f the fraction by volume of CO, η_{21} the rate coefficient for deactivation of the first vibrational level and $h\nu$ the vibrational quantum. This calculation was, however, based on a vibrational deactivation coefficient which was too large by many orders of magnitude. Recently McElroy et al. (1965) revised the earlier work and computed a temperature profile based on cooling from both the 1st vibrational and the rotational levels of CO. They concluded that vibrational transitions are insignificant and that radiation from the rotational levels of CO is the principal cooling mechanism. This calculation assumed a constant η which was obtained by extrapolation

from an experimental, high-temperature value. The full temperature dependence of the vibrational activation coefficient η_{12} is known from the theoretical considerations of several authors (Jackson and Mott, 1932; Schwartz and Herzfeld, 1954).

The solution of the problem given in Appendix B differs from that of these authors chiefly in the adoption of the scattering matrix point of view, as developed by Blatt and Biedenharn (1952) and employed by Arthurs and Dalgarno (1960) and Davison (1961) in connection with their treatment of rotational transitions. This treatment proves the inference of McElroy et al. (1965) that cooling by CO vibrational transitions is negligible in the Martian atmosphere, even when full temperature dependence is included.

The previously cited observational evidence (section 2) indicating a great abundance of CO₂ in the Martian atmosphere implies that radiative cooling by this constituent may be important. Chamberlain and McElroy (1966) have considered cooling by the ν_2 bands near 15μ in some detail, including the effect of reabsorption of radiation. They find the power radiated to be

$$3.33) \quad R_v(\text{CO}_2|z) = 1.9 \times 10^{-22} n_m n_{\text{CO}_2} e^{-(\theta/T) - (82.8/T)^{1/3}} \\ \times \left[1 - (1+\chi)e^{-\chi} \right] .$$

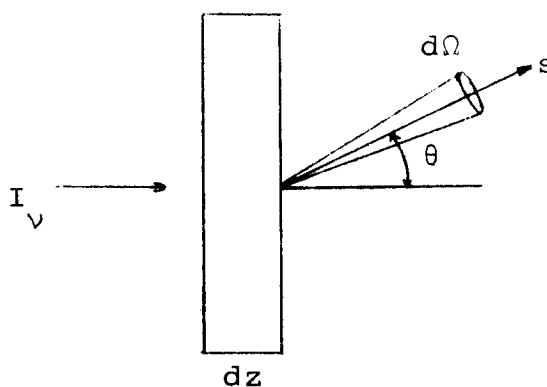
$\theta = h\nu/k = 725$ and $\chi = 1 \times 10^9 / n_{\text{CO}_2} (1 + A/n_m \eta)$, where A is the total transition probability and η the vibrational deactivation coefficient. The term in brackets on the right-hand-side of 3.33 is Chamberlain and McElroy's correction for reabsorption.

Optical Depth

Having obtained expressions for the source and radiative loss terms, the simplest procedure would be to substitute these in the thermal conduction equation 3.1 and integrate to find the temperature profile $T(z)$. This might lead to serious error. No provision has been made for the possibility that infrared photons, once emitted via one of the loss mechanisms just discussed, might be re-absorbed, and failure to take this into account will cause an overestimate of the loss terms, especially at lower altitudes. To account for the possibility of reabsorption we will suppose that radiative loss is ineffective

below the altitude at which radiation of the frequency considered would fall to e^{-1} of its initial value if it were incident at the top of the atmosphere and is completely effective above that level, i.e., we take unit optical depth in the atmosphere as the dividing line.

We will obtain an expression for the optical depth in a Doppler-broadened line from the equation of radiative transfer. Consider radiation of intensity I_ν quanta/cm² ster. incident on a slab of thickness dz containing n particles/cm³.



We wish to determine the change in beam intensity in the

direction specified by the element of solid angle $d\Omega$ due to emissions and absorptions between two energy levels which will be denoted by subscripts 2 (upper level) and 1 (lower level). The spontaneous emission occurs equally in all directions and is given by

$$3.34) \quad n_2 A_{21} \frac{d\Omega}{4\pi} ,$$

where n_2 is the number density of particles in the upper energy state, and A_{21} is the Einstein coefficient for spontaneous emission. The factor $d\Omega/4\pi$ is the fraction of emitted radiation which enters the solid angle $d\Omega$. Stimulated emission occurs in the direction of the incident beam and is given by

$$3.35) \quad n_2 B_{21} \rho_\nu ,$$

where B_{21} is the Einstein coefficient for stimulated emission and ρ_ν is the radiation density in the incident beam (quanta/cm³). The absorption is given by

$$3.36) \quad n_1 B_{12} \rho_\nu .$$

The decrease in the number of particles per unit time in the

upper energy level is $-dn_2/dt$. Each transition resulting in a decrease in n_2 corresponds to the addition of a photon to the radiation field. Since these photons are emitted over a finite frequency interval, the total decrease in n_2 corresponds to an increase in the photon intensity integrated over frequency and direction, i.e.,

$$3.37) \quad -\frac{dn_2}{dt} = \int d\Omega \frac{d}{ds} \int_0^\infty d\nu I_\nu .$$

The intensity of the radiation field is in general a broad function of frequency, but the change in this intensity due to the transitions considered here occurs over a narrow frequency interval. If the spectral line due to these transitions is Doppler-broadened and I_{ν_0} is the intensity in the frequency range $d\nu$ at the line center, we may write

$$3.38) \quad \int I_\nu d\nu = \int_0^\infty I_{\nu_0} e^{-[(\nu-\nu_0)/\alpha_D]^2} d(\nu-\nu_0) = \frac{\sqrt{\pi}}{2} \alpha_D I_{\nu_0} ,$$

where α_D is the Doppler width of the line. At the low pressures prevailing in the Martian thermosphere the 62μ oxygen line and the CO rotational lines will be Doppler broadened. Defining the photon flux by (where $\mu = \cos \theta$)

$$3.39) \quad F_\nu = \frac{1}{\pi} \int \mu I_\nu d\Omega$$

and equating the right hand side of 3.37 to the net decrease

in the number of particles in the upper energy state, we have (after substituting 3.38 and 3.39 in 3.37 and dropping the subscript o on ν)

$$3.40) \quad \frac{\sqrt{\pi}}{2} \alpha_D \frac{dF_\nu}{dz} = n_2 A_{21} + n_2 B_{21} \rho_\nu - n_1 B_{12} \rho_\nu \quad .$$

The energy density and intensity are related by

$$3.41) \quad \rho_\nu = \frac{1}{c} \int I_\nu d\Omega = \frac{4\pi}{c} \bar{I}_\nu$$

and the relations between the Einstein coefficients are

$$3.42) \quad \frac{B_{21}}{A_{21}} = \delta_\nu \quad , \quad \frac{B_{12}}{B_{21}} = \frac{g_2}{g_1} \quad ,$$

where δ_ν is a function of frequency to be specified later and g_2 and g_1 are the statistical weights of the upper and lower energy states. Using 3.41 and 3.42 the radiative transfer equation 3.40 may be written

$$3.43) \quad \frac{1}{4} \frac{dF_\nu}{dz} = \frac{1}{2\pi^{3/2}} \frac{A_{21}}{\alpha_D} n_2 \left[1 + \frac{4\pi\delta_\nu}{c} \left(1 - \frac{g_2}{g_1} \frac{n_1}{n_2} \right) \bar{I}_\nu \right] \quad .$$

If we assume the excited levels are thermally populated then

$$3.44) \quad \frac{n_1}{n_2} = \frac{g_1}{g_2} e^{\epsilon_{12}/kT} \quad \text{and} \quad n_2 = \frac{g_2}{z} e^{-\epsilon_2/kT} \quad ,$$

where z is the partition function and $\epsilon_{12} = \epsilon_1 - \epsilon_2$ with ϵ_1 and ϵ_2 the energies of states 1 and 2. The function δ_ν and the Doppler width α_D are given by (Goody, 1964)

$$3.45) \quad \frac{\delta_\nu}{c} = \frac{1}{8\pi} \left[\frac{c}{\nu} \right]^2, \quad \alpha_D = \frac{\nu}{c} \left[\frac{2kT}{m} \right]^{\frac{1}{2}},$$

where T is the temperature and m the particle mass.

Using 3.44 and 3.45 we may finally write the equation of transfer as

$$3.46) \quad \frac{1}{4} \frac{dF_\nu}{dz} = -\sigma_D n \bar{I}_\nu + \epsilon_D n,$$

where

$$3.47) \quad \sigma_D = \frac{1}{4\pi^{3/2}} \frac{g_2 A_{21}}{z(T)} \left[\frac{m}{2kT} \right]^{\frac{1}{2}} \left[\frac{c}{\nu} \right]^3 e^{-\epsilon_1/kT} \left[1 - e^{-\epsilon_{21}/kT} \right]$$

and

$$3.48) \quad \epsilon_D = \frac{1}{2\pi^{3/2}} \frac{g_2 A_{21}}{z(T)} \left[\frac{m}{2kT} \right]^{\frac{1}{2}} \left[\frac{c}{\nu} \right] e^{-\epsilon_2/kT}.$$

The ratio ϵ_D/σ_D is just the Planck function as would be expected since local thermodynamic equilibrium has been assumed. The quantity σ_D is the absorption cross section in the line. The optical depth τ is defined by

$$3.49) \quad d\tau = -\sigma_D n dz,$$

where dz is an increment of altitude and is taken in the vertical direction. If the constituent n is distributed in diffusive equilibrium in an isothermal atmosphere, the optical depth is

$$3.50) \quad \tau = \sigma_D n H \quad ,$$

and thus unit optical depth occurs at an altitude where the overlying number density is

$$3.51) \quad n H = \frac{1}{\sigma_D} \quad .$$

For the 62μ oxygen line we may evaluate the constants in 3.47 to find

$$3.52) \quad \sigma_D(0) = 8.9 \times 10^{-16} \frac{1 - e^{-228/T}}{5 + 3e^{-228/T} + e^{-325/T}} \frac{1}{T^{1/2}} \quad ,$$

and the overlying number density at unit optical depth, for $T = 300^\circ\text{K}$, is therefore

$$3.53) \quad (nH)_{\tau=1} = 2.4 \times 10^{17} \text{ cm}^{-2} \quad .$$

We recall our initial assumption that the atomic oxygen levels were in thermodynamic equilibrium which was in turn based on the assumption that radiation in the 62μ line was effective at altitudes where the total number density was $>10^9 \text{ cm}^{-3}$. That radiation does commence below this level is obvious from 3.53 since an atomic number

density of 10^9 would represent unit optical depth in the 62μ line only if the scale height were ≈ 1000 km.

In the case of carbon monoxide we are considering transitions between rotational states $J \rightarrow J-1$. We will take the optical depth in carbon monoxide to equal the optical depth in the rotational line in which most energy is transferred. Since the population of the J^{th} rotational state satisfies the proportionality

$$3.54) \quad n_J \propto (2J+1) e^{-\frac{\theta_r}{T} J(J+1)},$$

we readily find that the rotational state with the greatest occupation is specified by

$$3.55) \quad J_{\text{MAX}} = \left[\frac{T}{2\theta_r} \right]^{\frac{1}{2}}.$$

The Einstein coefficient for the transition $J \rightarrow J-1$ may be obtained by summing the right hand side of 3.12 over magnetic quantum states. We find

$$3.56) \quad A_{J,J-1} = \frac{4}{3h} (4\pi B)^3 d^2 \frac{J^4}{2J+1},$$

and with $J = J_{\text{MAX}}$ we have

$$3.57) \quad A = \frac{2^7 \pi^3}{3} \frac{B^3 d^2}{h} \left[\frac{T}{2\theta_r} \right]^{3/2} .$$

The absorption cross section in this case is

$$3.58) \quad \sigma_D(\text{CO}) = \frac{4\pi^{3/2}}{3\sqrt{e}} \frac{d^2}{h} \left[\frac{m}{kT} \right]^{1/2} \left[\frac{\theta_r}{T} \right]^{1/2} \left[1 - e^{-(2\theta_r/T)^{1/2}} \right] ,$$

or, to close approximation,

$$3.59) \quad \sigma_D(\text{CO}) = \frac{8\pi^{3/2}}{3\sqrt{e}} \frac{d^2}{h} \left[\frac{m}{kT} \right]^{1/2} \frac{\theta_r}{T} .$$

Evaluating the constants we find

$$3.60) \quad \sigma_D(\text{CO}) = \frac{1.35 \times 10^{-13}}{T^{3/2}} .$$

This expression was given by McElroy et al. (1965). At a temperature of $T = 300^\circ\text{K}$ unit optical depth occurs at an overlying density of

$$3.61) \quad (nH)_{\tau=1} \approx 3.8 \times 10^{16} \text{ cm}^{-2} .$$

Comparison of Total Flux Radiated by CO and O

As has been stated, comparison of the power radiated by O and CO does not provide a realistic comparison of the relative effectiveness of these constituents as cooling

agents. Comparison of the total flux radiated by each constituent will permit a more realistic evaluation of the relative importance of each radiator.

We will assume that in the radiation zone the scale height varies linearly so that

$$3.62) \quad H(z) = H_0 + \beta z \quad ,$$

where H_0 is the scale height at the bottom of the zone and β is the scale height gradient. The number density of a given constituent is then

$$3.63) \quad n(z) = \frac{n_0 T_0}{T(z)} e^{-\int_{z_0}^z \frac{dz}{H}} = \frac{n_0 T_0}{T(z)} \left[\frac{H_0}{H} \right]^{1/\beta} .$$

The optical depth is given by

$$3.64) \quad \tau(z_0) = -\int_{z_0}^{z_1} n(z) \sigma_D(T) dz \quad ,$$

where we assume that z_1 is the top of the radiating zone and that the optical depth above this level is negligible. Using 3.52 and 3.60 for the absorption cross sections in O and CO and 3.63 for the number density, we find the following expressions for the optical depths in these constituents:

$$3.65) \quad \tau(O) = \frac{\sigma_D^{(O)}(O)}{1 + \beta_{OX}/2} (n_0 H_0)_{OX} \left[1 - \Delta_{OX}^{(2+\beta_{OX})/2\beta_{OX}} \right]$$

$$3.66) \quad \tau(\text{CO}) = \frac{\sigma_{\text{D}_0}(\text{CO})}{1 + 3\beta_{\text{CO}}/2} (n_{\text{O}} H_{\text{O}})_{\text{CO}} \left[1 - \Delta_{\text{CO}}^{(2+3\beta_{\text{CO}})/2\beta_{\text{CO}}} \right],$$

where $\Delta = T_{\text{O}}/T_1$ and T_{O} , T_1 are the temperatures at the bottom and top of the radiating zone. The single subscript zero indicates the corresponding quantity is evaluated at z_0 . The subscripts OX and CO stand for atomic oxygen and carbon monoxide. The total flux radiated by each constituent (ergs/cm²sec) is given by

$$3.67) \quad F_{\text{R}} = \int_{z_0}^{z_1} R(z, T) dz,$$

where $R(z, T)$ is given by 3.29 for oxygen and 3.24 for CO. We find for the flux radiated by these constituents above an altitude z_0

$$3.68) \quad F_{\text{R}}(\text{O}) = 2.8 \times 10^{-18} (n_{\text{O}} H_{\text{O}})_{\text{OX}} f(T_{\text{O}}) \left[1 - \Delta_{\text{OX}}^{1/\beta_{\text{OX}}} \right]$$

$$3.69) \quad F_{\text{R}}(\text{CO}) = \frac{2.58 \times 10^{-23} (n_{\text{O}} T_{\text{O}}^2 H_{\text{O}})_{\text{CO}}}{1 - 2\beta_{\text{CO}}} \left[1 - \Delta_{\text{CO}}^{(1-2\beta_{\text{CO}})/\beta_{\text{CO}}} \right].$$

The slowly varying function $f(T_{\text{O}})$ in 3.69 was not included in the integration 3.67 but was removed from the integrand at the outset. The expression 3.69 was given by McElroy et al. (1965). The product $n_{\text{O}} H_{\text{O}}$ in 3.68 and 3.69 may be evaluated for $\tau = 1$ from 3.65 and 3.66. The total radiated flux is then

$$3.70) \quad F_{\text{R}}(\text{O}) = 9.6 \times 10^{-3} \left(1 + \frac{\beta_{\text{OX}}}{2} \right) E(T_{\text{O}}) T_{\text{O}}^{1/2} \left[\frac{1 - \Delta_{\text{OX}}^{1/\beta_{\text{OX}}}}{(2+\beta_{\text{OX}})/2\beta_{\text{OX}}} \right].$$

$$3.71) \quad F_R(\text{CO}) = 9.5 \times 10^{-11} \frac{2+3\beta_{\text{CO}}}{1-2\beta_{\text{CO}}} T_o^{7/2} \left[\frac{(1-2\beta_{\text{CO}})^{1-\Lambda_{\text{CO}}}}{(2+3\beta_{\text{CO}})^{1-\Lambda_{\text{CO}}}} \right]^{1/\beta_{\text{CO}}}$$

where $E(T_o) = 1/(e^{228/T_o} - 1)$.

It is of interest to note that the temperature dependence of the flux radiated is stronger than that of the power radiated. There are two distinct physical reasons for the temperature dependence of the radiated flux. One is the fact that the lines in which radiation occurs are Doppler broadened. As the temperature increases the absorption cross section in the center of a Doppler-broadened line falls off as $T^{-1/2}$ and this decrease in absorption cross section permits a photon emitted near the line center to escape more readily. The second temperature dependence results from the fact that, as the temperature of a region rises, the thermal population of the state or states from which radiation occurs increases and, conversely, the ground state population decreases. A photon traversing this region thus has a relatively greater chance of stimulating radiation from an upper state and a relatively smaller chance of being absorbed. This temperature dependence is also present in the expressions 3.52 and 3.58 for the absorption cross section in the center of the line. In each case this effect is responsible for, roughly, a $1/T$

dependence of the cross sections and is thus more important than the Doppler broadening. We could thus anticipate an approximate $T^{3/2}$ increase in temperature dependence of the total flux radiated by a constituent over the expression for the power radiated by the same constituent. This $T^{3/2}$ is present in the expressions 3.70 and 3.71 since, in 3.70 $E(T_o) \approx T_o$ for $T_o \gtrsim 300^\circ\text{K}$.

If we neglect the difference in temperature at unit optical depth in atomic oxygen and carbon monoxide and assume T_o refers to the temperature at which carbon monoxide begins to radiate, then the ratio of the total heat fluxes radiated by O and CO is

$$3.72) \quad R = \frac{F_R(O)}{F_R(CO)} = 5 \times 10^7 \frac{(2+\beta_{OX})(1-2\beta_{CO})}{(2+3\beta_{CO})} \frac{E(T_o)}{T_o^3} \\ \times \frac{\left[1-\Delta_{OX}^{1/\beta_{OX}}\right] \left[1-\Delta_{CO}^{(2+3\beta_{CO})/2\beta_{CO}}\right]}{\left[1-\Delta_{OX}^{(2+\beta_{OX})/2\beta_{OX}}\right] \left[1-\Delta_{CO}^{(1-2\beta_{CO})/\beta_{CO}}\right]} .$$

This ratio is plotted as a function of temperature at the bottom of the radiation zone in Fig. 6. The curves are labelled according to the assumed value of β_{OX} . In the Martian atmosphere $\beta_{OX} = .1$ corresponds to a temperature gradient of about 2°K/km . It is clear that atomic oxygen may be an important radiator in the Martian atmosphere under

a wide range of temperature conditions. If the temperature at the bottom of the radiation zone is less than 300°K atomic oxygen can be the principal radiator. The transition temperature at which O and CO radiate equal fluxes depends on the values of β_{OX} and β_{CO} in the radiation zone. Even for temperatures $T_{\text{O}} \approx 500^{\circ}\text{K}$ atomic oxygen radiates roughly 25% of the total flux radiated by CO and O. This of course presumes roughly equal temperatures at unit optical depth in the CO and O. The error caused by this assumption is approximately $[T_{\text{O}}(\text{O})/T_{\text{O}}(\text{CO})]^{\frac{1}{2}}$ in 3.72, where $T_{\text{O}}(\text{O})$ is the temperature at unit optical depth in O and $T_{\text{O}}(\text{CO})$ the temperature at unit optical depth in CO.

Thermospheric Heating

The most important source of heating in the upper atmosphere is provided by absorption of solar ultraviolet radiation. The exact mechanisms by which the ultraviolet photon energy is transformed into kinetic energy of the atmospheric particles is not well understood at present and this lack of knowledge is generally incorporated into a heating efficiency factor ϵ , which appears in the q of 3.2. The simplest form which can be adopted for $q(z,t;T)$ is

$$3.73) \quad q(z) = \frac{1}{2} F_{\infty} \epsilon_0 N(z) e^{-\tau/\mu} ,$$

where F_{∞} is the solar flux at the top of the atmosphere, ϵ the efficiency of heating, σ the absorption cross section, $N(z)$ the atmospheric density, τ the optical depth, and μ the cosine of an effective solar zenith angle. The factor $1/2$ allows for planetary rotation. F_{∞} , σ , and presumably ϵ are all functions of wavelength, and in the form in which they appear in 3.73 they must be considered as averaged quantities. The optical depth is defined by $d\tau = -N(z)\sigma dz$. The exponential factor in 3.73 thus represents the effect of absorption above the altitude under consideration. The form 3.73 of q does have the advantage of being integrable and if a sufficiently simple approximation for L were found a first integral of 3.1 could be obtained. An improved form of $q(z)$ is provided by assuming that F_{∞} , σ , and ϵ are averaged over short wavelength intervals rather than over the entire spectrum so that $q(z)$ is

$$3.74) \quad q(z) = \frac{1}{2} \sum_i (F_{\infty})_i \epsilon_i \sigma_i N(z) e^{-\tau_i/\mu}.$$

The effect of different absorption cross sections, σ_i , in different wavelength intervals is to spread the heating term $q(z)$ over a wider range of altitudes.

For a preliminary estimate of the heating rate in the

Martian thermosphere we will adopt the functional form of 3.73 for $q(z)$. If the ionizable constituent is atomic oxygen and a diffusive distribution is assumed, then the heating rate due to photoionization is

$$3.75) \quad q(z) = \frac{1}{2} F_{\infty}(\lambda) \sigma(\lambda) \epsilon n_0 e^{-(z/H_0) - n_0 \sigma H_0 \sec \chi} e^{-z/H_0},$$

where H_0 is the atomic oxygen scale height, χ is the solar zenith angle, and z is the altitude measured from the height at which the oxygen density is n_0 . By differentiating the argument of the exponential factor on the right-hand-side of 3.75 we find that the heat input occurs at an altitude of

$$3.76) \quad z_m = H_0 \ln n_0 \sigma H_0 \sec \chi,$$

and since z_m is measured relative to n_0 we see that the number density of atomic oxygen at the altitude of maximum heating is

$$3.77) \quad n_m = \frac{\cos \chi}{\sigma H_0}.$$

Taking a mean photoionization cross section of $\sigma = 10^{-17} \text{ cm}^2$ estimated from the paper of Hinteregger et al. (1965), a

scale height $H_0 = 20$ km , and a solar zenith angle of 67° , corresponding to that at Mariner imersion, we obtain

$$3.78) \quad n_m = 7.0 \times 10^{10} \text{ cm}^{-3}$$

as an estimate of the oxygen number density in the region of maximum heating.

The extreme ultraviolet (EUV) flux incident at the top of the atmosphere in the wavelength region below 911\AA can be obtained from various sources. However, the most that can be said for our knowledge of this flux is that it is correct to within approximately $\pm 30\%$. Hinteregger et al. (1965) estimate, for example, that their flux data are accurate to a factor of 3 to 5 for short wavelengths and to $\pm 30\%$ above 250\AA . The thermospheric temperature is quite sensitive to the EUV flux and this quantity must be regarded as the principal uncertainty in determining the temperature.

Table 2 gives the EUV flux data of Hinteregger et al. (1965). The photoionization cross sections for the constituents present in the Martian atmosphere are also given. The values for O, O₂ and N₂ are from Hinteregger's paper, and the values for CO and CO₂ are estimated from the data of Schultz, Holland and Marmo (1963). At short wavelengths, where photoionization cross sections for CO and CO₂ were not available, the CO cross sections have been set equal to those

Table 2

Flux and Cross Section Data

λ	F_E (erg/cm ² sec)	σ_O (10 ⁻¹⁸) cm ²	σ_{CO} (10 ⁻¹⁸) cm ²	σ_{N_2} (10 ⁻¹⁸) cm ²	σ_{O_2} (10 ⁻¹⁸) cm ²	σ_{CO_2} (10 ⁻¹⁸) cm ²
1027-990	.049				0.90	
1025.7	.045				0.76	
991.5	.007				0.76	
990-950	.021				4.0	
977.0	.081				1.6	
972.5	.011				18.	
950-920	.022				4.2	
949.7	.005				3.0	
937.8	.004				2.9	
920-911	.028				4.8	
911-890	.089				7.9	
890-860	.096	2.7	11.		6.2	22.
860-840	.047	2.9	22.		5.3	22.
840-810	.048	3.1	23.		9.1	12.
832-835	.013	3.2	23.		5.4	12.
810-796	.017	3.3	29.		14.	14.
796-780	.019	3.3	31.	14.3	13.9	26.
790.1	.003	3.3	31.	14.0	13.7	13.
787.7	.008	3.3	31.	4.9	11.2	26.8
780.3	.004	3.3	31.	7.6	16.8	24.4
780-760	.019	3.4	31.	14.5	11.2	38.
770.4	.011	3.4	31.	8.3	10.2	38.6

Table 2 (continued)

λ	F_E (erg/cm sec)	σ_O (10^{-18}) cm ²	σ_{CO} (10^{-18}) cm ²	σ_{N_2} (10^{-18}) cm ²	σ_{O_2} (10^{-18}) cm ²	σ_{CO_2} (10^{-18}) cm ²
765.1	.006	3.4	31.	49.	13.9	74.5
760-740	.013	3.4	26.	17.7	13.	29.
740-732	.005	3.5	26.	17.4	29.	21.
732-700	.015	7.7	29.	20.	25.	21.
703.8	.007	8.1	29.	23.	23.	21.
700-665	.020	8.3	26.	24.	22.	24.
665-630	.017	11.5	26.	25.	31.	26.
630-600	.039	12.5	25.	22.	37.	30.
629.7	.028	12.0	26.	23.	33.	30.
625.0	.028	12.0	20.	23.	33.	30.
600-580	.053	13.	18.5	21.	25.	33.
584.3	.053	13.	18.5	21.	28.	28.2
580-540	.050	13.	19.1	22.	26.	33.
540-510	.018	13.	19.1	23.	26.	33.
510-500	.041	13.	19.1	22.	25.	33.
500-480	.042	12.9	18.5	21.	24.	28.5
480-460	.030	12.1	18.1	21.	23.	28.5
460-435	.022	10.5	17.5	19.8	23.	24.
435-400	.047	12.5	17.0	17.0	24.	23.5
400-370	.029	11.1	16.0	13.1	23.	26.5
370-355	.050	10.0	15.0	10.6	22.	26.5
368.1	.031	10.3	15.0	11.3	22.	27.9
355-340	.044	9.3	14.2	9.1	22.	22.
340-325	.045	8.7	14.2	7.7	21.	21.
325-310	.047	8.1	8.1	6.4	20.	21.

Table 2 (continued)

λ	F_E ($\text{erg}/\text{cm}^2 \text{ sec}$)	σ_O (10^{-18}) cm^2	σ_{CO} (10^{-18}) cm^2	σ_{N_2} (10^{-18}) cm^2	σ_{O_2} (10^{-18}) cm^2	σ_{CO_2} (10^{-18}) cm^2
310-280	.113	9.2	9.2	4.9	18.7	22.
303.8	.250	9.8	9.8	4.1	19.5	14.1
280-260	.062	8.0	8.0	4.2	16.0	23.
260-240	.064	6.7	6.7	3.6	13.4	22.5
257.0	.011	7.2	7.2	3.8	14.4	26.
256.3	.012	7.2	7.2	3.8	14.4	26.
240-220	.081	5.6	5.6	3.1	11.2	22.
220-205	.059	4.7	4.7	2.8	9.4	22.
205-190	.163	4.0	4.0	2.4	8.0	19.
190-180	.250	3.4	3.4	2.2	6.8	15.4
180-165	.371	2.9	2.9	1.9	5.7	15.4
165-138	.092	2.1	2.1	1.4	4.2	15.4
138-103	.099	1.1	1.1	0.90	2.2	4.4
103-83	.149	0.7	0.7	0.55	1.4	2.8
83-62	.137	0.4	0.4	0.37	0.80	1.6
62-41	.135	0.22	0.22	0.18	0.44	0.88
41-31	.083	0.10	0.10	0.07	0.20	0.40
31-22.8	.004	0.50	0.50	1.00	0.09	0.18
22.8-15	.003	0.35	0.35	0.36	0.70	1.40
15-10	.001	0.14	0.14	0.15	0.27	0.54
10-5	.001	0.04	0.04	0.04	0.08	0.16

The flux values at the top of the Earth's atmosphere, F_E , and the O , O_2 , and N_2 cross sections are from Ginteregger *et al.* (1965). The CO and CO_2 cross sections are estimated from Schultz, Holland and Marmo (1963).

for O and the CO_2 to twice the O_2 cross sections. The flux values in the wavelength intervals given in Table 2 exclude the energy flux in the strong spectral lines. The values for the lines are given separately. The small interval 832-835 \AA in Table 2 gives the flux in the O II, III lines.

In addition to possible uncertainties in the data, the EUV flux itself is variable over a solar cycle and the correct flux values observed at one time might not be appropriate for thermospheric computations at another. The Mariner IV observations were made at a time of minimum solar activity and we should therefore expect relatively low values of solar flux to give temperatures in agreement with observation.

Sources of heating other than the solar EUV below 1100 \AA could be considered. The wavelength region between 1100 \AA and 1800 \AA dissociates both O_2 and CO_2 . The magnitude of this dissociative heating in the Schumann-Runge region has been estimated for the Earth's atmosphere by Walker (1964) and taken into explicit account by Harris and Priester (1964). Harris and Priester find that this dissociative heating (which occurs mostly at altitudes below 120 km) does not greatly influence the exospheric temperature. In the Martian atmosphere this heating will occur predominately in the 70-90 km altitude region and is thus unlikely to

significantly increase the exospheric temperature.

The heating which occurs when the dissociated products recombine may also be considered. For example, from 2.3 we see that this heat source for atomic oxygen recombination to form O_2 may be written

$$3.79) \quad q_{RC}(z) = k_2 \Delta E n_M(z) n_O^2(z) \quad .$$

Since atomic oxygen is the dominant thermospheric constituent we may estimate this source as

$$3.80) \quad q_{RC}(z) \approx 2 \times 10^{-44} n_O^3(z) \text{ ergs/cm}^3 \text{ sec} \quad ,$$

where $\Delta E = 5.1 \text{ e.v.}$ (Wray, 1961) has been used for the energy release on recombination, and the rate coefficient $k_2 = 2.7 \times 10^{-33} \text{ cm}^6/\text{sec}$ (Barth, 1964). At the altitude of maximum solar EUV heating, $n_O(z) \approx 10^{11}$ at most, and this heat source is thus of the order of $10^{-11} \text{ ergs/cm}^3 \text{ sec}$, which is negligible compared with the roughly $10^{-8} \text{ erg/cm}^3 \text{ sec}$ contributed by solar EUV. At lower altitudes, i.e., in the 70-90 km region, this heating could be significant, but again this will not increase the exospheric temperature. Equation 3.79 has, of course, assumed that all of the 5.1 e.v. available on recombination goes into heating the ambient gas

and has completely neglected radiative loss in the atmospheric bands of O_2 . The above discussion thus overestimates the magnitude of the recombination heating.

Since some of the model thermospheres studied in this paper have temperatures at ionospheric altitudes which are about the same as or colder than temperatures in the lower atmosphere, the possibility of radiative heating of the upper atmosphere by the planetary spectrum must be considered. Such heating cannot be significant for the models studied in this paper however. In all the models studied unit optical depth in atomic oxygen and carbon monoxide occurs above 100 km (usually above 110 km), dissociation of CO_2 occurs near 80 km, and the scale height in this region is about 5-10 km. There are thus several optical thicknesses of these radiating constituents below ionospheric altitudes and any radiative exchange with the ground must occur in the same altitude interval where CO_2 dissociation occurs.

Only the solar EUV heating is explicitly used in these model studies. This, of course, involves the basic assumption that the temperature of the thermosphere reflects the heating and cooling processes which occur in the thermosphere and that this temperature is not significantly altered by heating at much lower altitudes. The heat input near mesopause altitudes is implicit in the boundary temperature assumed at

the mesopause, and it has been found that the exospheric temperature is insensitive to variation in conditions at the lower boundary. The assumption of heating by solar EUV alone leads to successful description of the time-averaged temperature structure in the Earth's thermosphere (Hunt and van Zandt, 1961; Lazarev, 1964).

Heating Function Used in Present Calculation

The solar EUV heat source appearing in the thermal conduction equation has been computed from

$$3.81) \quad Q(z) = \frac{e}{2} \sum_{j=1}^5 n_j(z) \sum_i F_{\infty}(\lambda_i) \sigma_j(\lambda_i) e^{-\frac{1}{\mu} \sum_{k=1}^5 \sigma_k(\lambda_i) \int_z^{\infty} n_k(z) dz}$$

where the sums \sum_j and \sum_k are taken over the five constituents CO_2 , CO , O_2 , N_2 and O , and the sum \sum_i is the sum over the wavelength intervals given in Table 2.

Integration of the Thermal Conduction Equation

Having found functional forms for the thermospheric heating and cooling mechanisms we turn to a derivation of the temperature profile. This is accomplished via numerical integration of the thermal conduction equation which we write in the time-independent form

$$3.82) \quad \frac{d}{dz} \left[K(z, T) \frac{dT}{dz} \right] + q(z) - L(z, T) = 0 \quad .$$

$q(z)$ is the rate of heat generation (ergs/cm³sec) given by 3.74 and $L(z, T) = R_s + R_r + R_v$ is the sum of the heat losses. R_s , R_r , and R_v are given by equations 3.29, 3.24, and 3.33. The temperature dependence of the thermal conductivity may be written (Nicolet, 1960)

$$3.83) \quad K(z, T) = K_o(z) T^{\frac{1}{2}} \quad .$$

The dependence of K on altitude is a result of the variation of composition with height. The conductivity K_o is computed by taking an average, at each altitude, of the individual conductivities of the constituents CO_2 , CO , O_2 and O weighted by the fraction of the constituent present at that altitude. The conductivities of CO_2 , CO , and O_2 are taken from the tables on pages 574 and 577 of Hirschfelder, Curtiss, and Bird (1954) and that of O is from Nicolet (1960). The values of the conductivities used are given in Table 3.

With the change of variable $U = T^{3/2}$, the thermal conduction equation 3.82 can be reduced to the following two first order differential equations:

Table 3

Thermal Conductivities of Species Present in the Martian Thermosphere.

<u>Constituent</u>	$K \times 10^7$ (cal/cm sec °K)	at T (°K)	$K_O \times 10^{-4}$ (erg km/cm ² sec °K ^{1/2})	<u>Reference</u>
CO ₂	227	200	6.7	HCB
O ₂	216	100	9.0	HCB
CO	530	273.16	13.4	HCB
N ₂	550	273.16	13.9	HCB
O	-	-	36.0	N

$$K(z, T) = K_O(z) T^{\frac{1}{2}}$$

References: HCB - Hirschfelder, Curtiss, and Bird (1954, pp. 574 and 577).

N - Nicolet (1960).

$$3.84) \quad K_o(z) \frac{dP}{dz} + K'_o(z)P = - \frac{3}{2} Q(z,U)$$

$$3.85) \quad \frac{dU}{dz} = P \quad ,$$

where $K'_o(z) = dK_o(z)/dz$ and $Q(z,U) = q(z) - L(z,U)$ is the net rate of heat generation. These have been integrated simultaneously on an IBM 360 (Mod. 75) computer at the Goddard Institute for Space Studies for a range of atmospheric compositions. The method used was a standard Runge-Kutte procedure (Kuo, 1965, Chapter 7).

The equations 3.84 and 3.85 are integrated upward from an arbitrarily chosen altitude which has been varied between 70 and 90 km for these model studies. One boundary condition is taken as $dT/dz = 0$ and this is held fixed, which means that the altitude at which integration is begun is assumed to be the mesopause for the model under consideration. The temperature at the boundary is then varied until an isothermal profile is obtained at high altitudes. The nature of the solutions obtained can be studied by writing 3.82 in the form

$$3.86) \quad \frac{d^2 T^{3/2}}{dz^2} = - \frac{3}{2K_o} [q(z) - L(z,T)] \quad .$$

The altitude dependence of the thermal conductivity has been neglected to simplify the discussion.

In a region where radiative cooling is greater than the heat input, the right-hand-side of 3.86 is positive and the temperature gradient $dT^{3/2}/dz$ will increase with altitude. In regions where $q > L$ the temperature profile will bend over as the gradient becomes smaller. Since the heating term $q(z)$ is only weakly temperature-dependent, whereas $L(z, T)$ increases with T , we can readily ascertain the type of solutions to which 3.86 gives rise. We assume that the Martian exosphere is isothermal as is the Earth's and that the solution we seek is characterized by a zero temperature gradient at high altitude.

Suppose we choose too high a temperature T_1 , say, at the mesopause (Fig. 7). The values of $L(z, T)$ will then be too large and the run of temperatures will be too high with a positive gradient at high altitudes. This is illustrated by curve A in Fig. 7. On the other hand, if we choose too low a temperature T_3 the cooling will be insufficient and the temperature run will be driven negative, as shown by curve B. The correct boundary temperature T_2 will give a profile of the assumed form, such as C.

The actual conditions of density and temperature at the mesopause are largely determined by the processes of

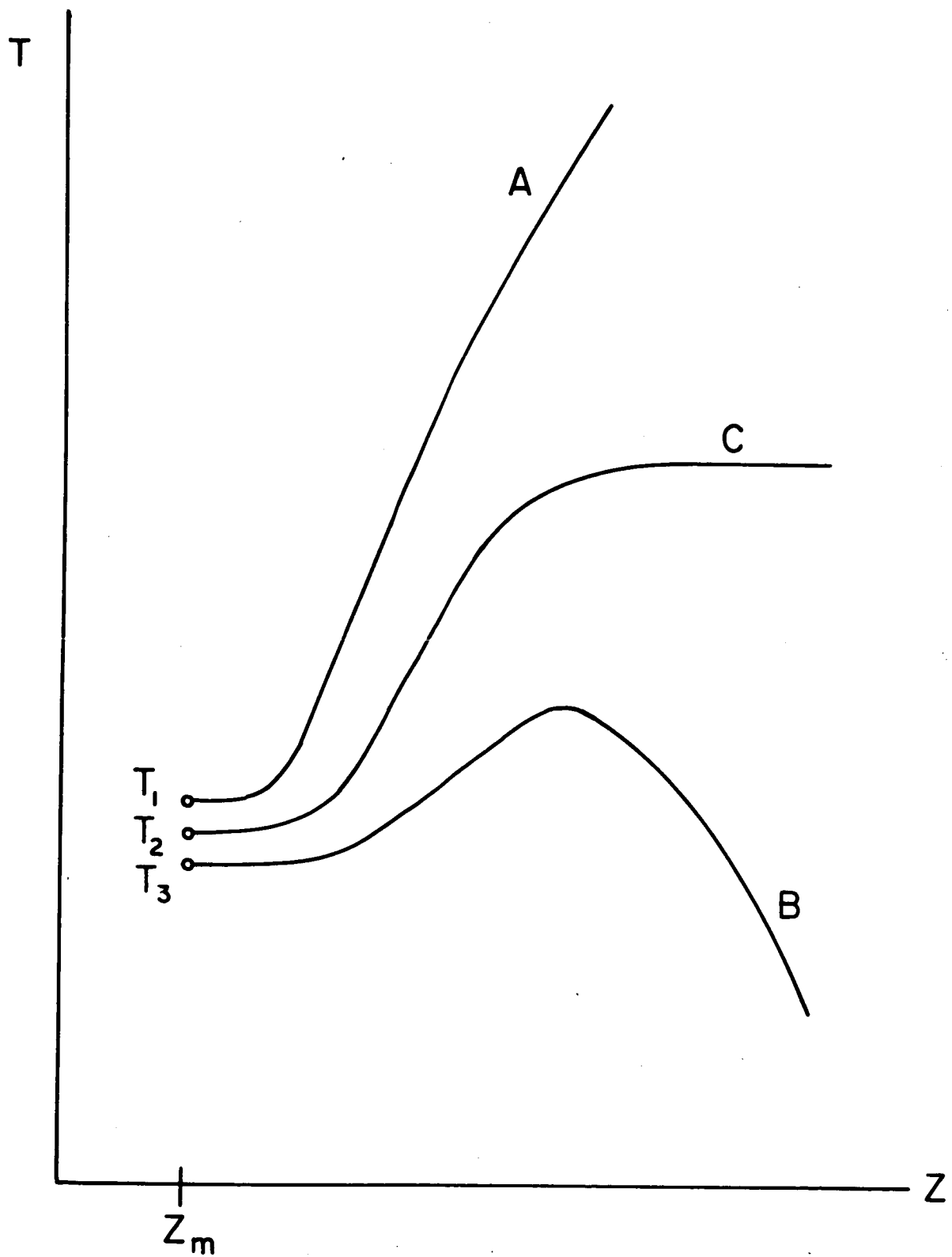


Fig. 7. Mathematical solutions of the thermal conduction equation for boundary conditions $\left[\frac{dT}{dz}\right]_{z=z_m} = 0$ and $T(z_m) = T_1, T_2, T_3$.

heat deposition and transport occurring between the ground and mesopause altitude. Therefore, our calculation concerns only the altitudes above the mesopause and does not determine the mesopause altitude or temperature. The altitude and temperature at the mesopause are boundary conditions in our formulation of the upper atmosphere problem. We have found that our main result, the temperature in the Martian exosphere, is insensitive to variations in these boundary conditions over the altitude range from 70 to 90 km that has been studied. Uncertainties in the values of the boundary conditions are therefore not a difficulty. In practice, a ten kilometer increase in mesopause altitude resulted in roughly a 5°K increase in exosphere temperature for the models studied here. The models can therefore be matched to a higher run of temperatures in the assumed mesopause region by increasing the altitude at which integration is begun, and the exospheric temperature will be little changed by such a procedure.

To obtain rigorously correct solutions the thermal conduction equation 3.82 would have to be integrated simultaneously with the equations of continuity for each molecular species present (equations A.12 of Appendix A). Since our primary interest is in finding the temperatures and not the densities, there are two reasons why this is not essential.

First, the exospheric temperature has been found to vary by only about 50°K (roughly 20%) for the most extreme density models studied (with a fixed solar flux), i.e., for an atmosphere in which the CO_2 is highly dissociated to low altitudes and one in which it is only slightly dissociated beginning at 70 km. Physically, this results from the fact that changing the extent of dissociation and the altitude at which it occurs alters the location of the heat source and radiative sinks in the atmosphere, but changes their relative locations and their magnitudes only slightly. Increasing the extent of dissociation raises the mesopause altitude and the altitudes at which heating and cooling are effective. Second, it has been found that the numerical solutions of the conduction equation can be approximated quite well by a functional form

$$3.87) \quad T(z) = T_M + (T_{\infty} - T_M) (1 - e^{-z^2/A}) \quad ,$$

where T_M is the mesopause temperature, T_{∞} the exospheric temperature, z the altitude above the mesopause, and the constant A may be chosen to match the numerical solution and 3.87 at any selected point.

The densities used in evaluating the heating and loss terms in 3.82 are calculated from the equation

$$3.88) \quad n(z) = n_o \frac{T_o}{T(z)} e^{-\int_z^{\infty} dz/H},$$

where $H = kT(z)/mg(z)$ is the scale height and $T(z)$ is given by 3.87. Once a successful solution such as C in Fig. 6 is obtained, new parameters T_M , T , and A may be chosen to fit this solution and integration of the thermal conduction equation carried through again. This procedure could be repeated several times, but in practice a close fit is obtained between 3.87 and the solution of 3.82 on the third integration. Actually, the exospheric temperature changes by only a few degrees from the value obtained on initial integration of the conduction equation even for a poor first estimate of T_M , T , and A , which again substantiates the finding that this temperature is relatively insensitive to the density distributions.

The results of integrating the conduction equation for EUV heating fluxes varying from .15 to .55 erg/cm²sec are presented in Fig. 2. The flux values at which carbon monoxide cooling becomes dominant is indicated by the vertical bar. Since the total flux radiated by carbon monoxide is proportional to $T^{7/2}$ the portion of the curve corresponding to higher flux values is flatter than the lower part where atomic oxygen cooling predominates.

Figure 3 is a plot of the temperature of the Martian exosphere during the solar cycle using the 1954-1965 cycle as typical. The variation of the 10.7 cm solar flux during this period ranged from roughly 70 to 250 (10^{-22}) watts/ m^2 cps (Harris and Priester, 1962), corresponding to a probable variation in the mean solar EUV at Mars of .26 to .92. The upper curve of Fig. 3 shows the variation of the mean temperature of the Earth's thermosphere during the solar cycle (Harris and Priester, 1962). Since the carbon monoxide content of the Earth's upper atmosphere is negligible, there is no effective thermostat keeping the temperature down as the heat input increases. The variation with solar cycle of the Earth's exospheric temperature is thus relatively much greater than the variation for Mars.

From Fig. 3 we see that the temperature of the Martian exosphere will always be below the 1100°K that would be necessary for the thermal escape of atomic oxygen. Heavier inert gases such as neon and argon would also be retained. The temperature does, however, become great enough for the lighter gases such as hydrogen and helium to escape. Hydrogen cannot be retained by Mars at exospheric temperatures above 70°K and the corresponding value for helium escape is 275°K .

THE IONOSPHERE

The physical processes responsible for the formation of regions of ionization in a planetary atmosphere are well understood. An extensive review of ionospheric theory has been given by Yonezawa (1965). In the following, the mechanisms responsible for layer formation will be discussed, and the type of ionization layer in best accord with the Mariner observation will be considered.

The existence of an ionized layer is determined by the competition between electron production and loss. Identification of the chemical reaction responsible for electron loss is of primary importance in determining whether diffusive loss must be considered. In the development of the theory, reference will often be made to the situation in the Earth's ionosphere. It is felt that this will best serve to clarify the arguments and prepare for their application to Mars.

The presence of charged particles in the upper atmos-

phere arises as a consequence of the ionization by the solar extreme ultraviolet radiation of the neutral constituents present there. Since the energy required for ionization of atomic or molecular constituents is generally greater than that required for molecular dissociation, the wavelengths of interest for the ionosphere are shorter than those relevant to CO_2 photolysis. The upper limit to the wavelength of radiation capable of ionizing atomic oxygen, for example, is 911\AA , and the maximum ionization cross section occurs between 500\AA and 600\AA . Ionization cross sections vary differently with wavelength for different atmospheric constituents, giving rise to the appearance of local electron production maxima at different altitudes and, hence, to the existence of ionospheric layers.

If $F(\lambda, z)$ denotes the solar flux of wavelength λ at altitude z , with $n_i(z)$ the number density of the i^{th} ionizable constituent, and $\sigma_i(\lambda)$ the cross section for ionization of n_i at wavelength λ , then the rate of electron production at height z may be written

$$4.1) \quad Q_e(z) = \sum_{\lambda, i} \gamma_i F(\lambda, z) \sigma_i(\lambda) n_i(z) \quad ,$$

where γ_i is the number of electron-ion pairs formed per absorbed photon -- photoionization yield -- and the summation

over λ is understood to be over the values of the wavelength-dependent quantities in discrete wavelength intervals. If $F_{\infty}(\lambda)$ is the solar flux at the top of the atmosphere, the attenuation of the radiation as it penetrates the atmosphere may be expressed by

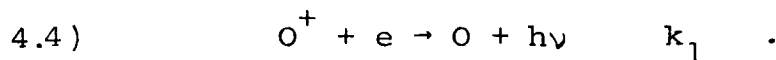
$$4.2) \quad F(\lambda, z) = F_{\infty}(\lambda) e^{-\sum_j \sigma_j(\lambda) \int_z^{\infty} n_j(z) dz / \mu}$$

where μ is the cosine of the solar zenith angle. If we assume that the region of ionization is isothermal and that there is only one ionizable constituent, 4.1 and 4.2 may be combined as

$$4.3) \quad Q_e(z) = \sum_{\lambda} \gamma F_{\infty}(\lambda) \sigma(\lambda) n_o e^{-\frac{z}{H} - n_o \sigma(\lambda) H \sec \chi} e^{-z/H}$$

where H is the neutral atmospheric scale height, and χ is the solar zenith angle. The altitude z is measured above some reference level in the atmosphere at which $n = n_o$.

The form of the electron density profile depends on the assumptions made regarding the loss mechanism. The simplest assumption would be a loss via radiative recombination



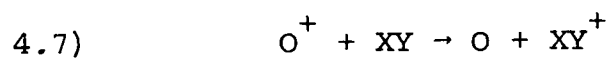
The rate constant is $k_1 = 4 \times 10^{-12} \text{ cm}^3/\text{sec.}$ at 250°K (Biondi, 1964). The loss rate is then

$$4.5) \quad L = k_1 n_{\text{O}^+} n_{\text{e}} = k_1 n_{\text{e}}^2 ,$$

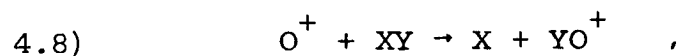
and if photochemical equilibrium is assumed, the density profile is

$$4.6) \quad n_{\text{e}}(z) = \sqrt{\frac{Q_{\text{e}}(z)}{k_1}} .$$

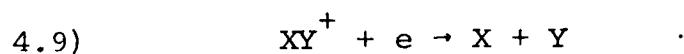
The ionospheric layer described by 4.6 is known as a Chapman layer. It exhibits an absolute maximum in electron density at the same altitude as the maximum in the production function Q_{e} . The observed maximum electron density in the Earth's ionosphere is less than the maximum density value in a Chapman layer, and it occurs at a higher altitude. Hence, 4.6 does not provide a good description of the Earth's ionosphere. The inadequacy in this model is in the assumption of radiative recombination as the sole loss mechanism. The presence of molecular constituents provides alternative and more rapid mechanisms by which electrons may be lost. For example, a molecule XY may first acquire a charge via a charge exchange or ion-atom interchange reaction



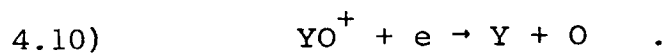
or



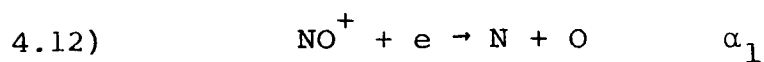
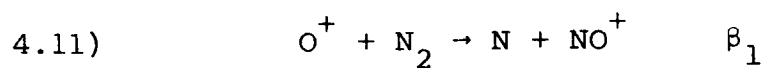
this being followed by dissociative recombination



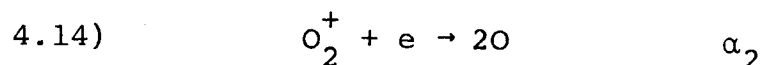
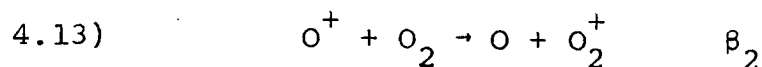
or



In the Earth's ionosphere the dominant molecular species are N_2 and O_2 , and the following set of reactions might be postulated for electron removal:



and



The α 's and β 's are the rate coefficients for the reactions. An ion-atom interchange reaction has been written for 4.11 since this type of reaction has been generally observed to proceed more rapidly than charge exchange. The consequences of reactions 4.11-4.14 for the shape of the electron density profile have been discussed by Yonezawa (1965); the main points of his review are reiterated below.

The form of the loss function depends upon whether the loss is limited by the ion-atom interchange reactions 4.11 and 4.13 or by the dissociative recombination reactions 4.12 and 4.14. The former would be expected to limit the loss at higher altitudes due to the decreasing availability of the molecular constituents, whereas the latter will limit the loss at lower altitudes due to the smaller electron density. These removal mechanisms are said to be the attachment type (high altitudes) and the recombination type (low altitudes), and the rates may be written, respectively

$$4.15) \quad L_a = (\beta_1 n_{\text{N}_2} + \beta_2 n_{\text{O}_2}) n_{\text{O}^+}$$

$$4.16) \quad L_r = (\alpha_1 n_{NO^+} + \alpha_2 n_{O_2^+}) n_e ,$$

or

$$4.17) \quad L_a = \beta_{eff} n_e$$

$$4.18) \quad L_r = \alpha_{eff} n_e^2 ,$$

where

$$4.19) \quad \beta_{eff} = \beta_1 n_{N_2} + \beta_2 n_{O_2}$$

is the effective attachment coefficient, and

$$4.20) \quad \alpha_{eff} = \frac{\alpha_1 n_{NO^+} + \alpha_2 n_{O_2^+}}{n_{NO^+} + n_{O_2^+}}$$

is the effective recombination coefficient. The condition of charge neutrality, $n_e = n_{O^+}$ at high altitudes and $n_e = n_{NO^+} + n_{O_2^+}$ at low altitudes, has been used in 4.17 and 4.18. By equating the rates of production and loss of the molecular ions in 4.11-4.14, we find readily that

$$4.21) \quad \frac{n_{\text{NO}^+}}{n_{\text{O}_2^+}} = \frac{\frac{\beta_1}{\alpha_1} n_{\text{N}_2}}{\frac{\beta_2}{\alpha_2} n_{\text{O}_2}},$$

and the effective recombination coefficient can be written

$$4.22) \quad \alpha_{\text{eff}} = \frac{\beta_1 n_{\text{N}_2} + \beta_2 n_{\text{O}_2}}{\frac{\beta_1}{\alpha_1} n_{\text{N}_2} + \frac{\beta_2}{\alpha_2} n_{\text{O}_2}},$$

which is approximately independent of altitude. The electron density profiles in regions governed by attachment-type and recombination-type loss are thus described by

$$4.23) \quad n_e = \frac{Q_e}{\beta_{\text{eff}}} \quad \text{attachment-type loss}$$

and

$$4.24) \quad n_e = \sqrt{\frac{Q_e}{\alpha_{\text{eff}}}} \quad \text{recombination-type loss}.$$

The production function Q_e may be written

$$4.25) \quad Q_e(z) = Q_0 e^{1 - [(z-z_0)/H] - (\sec \chi) e^{-(z-z_0)/H}},$$

where, it will be recalled, z_0 is the altitude of maximum electron production and H is the scale height of atomic oxygen. At high altitudes $z \gg z_0$, Q_e decreases as

$-(z-z_o)/H$
 e ; however, β_{eff} , given by 4.19 falls off with a scale height corresponding to N_2 . H_{N_2} is less than H , and therefore the electron profile of 4.23 is a monotonically increasing function at high altitudes, and the ionization layers having a loss mechanism described by 4.11-4.14 can exhibit no absolute maximum. If the profiles described by 4.23 and 4.24 are combined at the altitude where the attachment- and recombination-type loss rates are equal, i.e., at an altitude where (equating the right hand sides of 4.17 and 4.18)

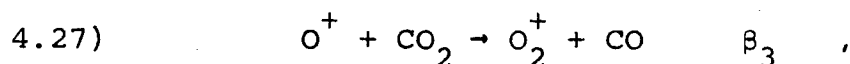
$$4.26) \quad \frac{\beta_1}{\alpha_1} n_{N_2} + \frac{\beta_2}{\alpha_2} n_{O_2} = n_e ,$$

a local maximum may still be exhibited. Since α_{eff} is approximately independent of height, the condition for a local maximum in the electron density profile is that there be a local maximum in the production function Q_e occurring at an altitude where the recombination-type loss is dominant.

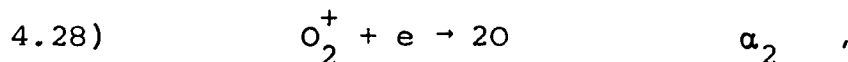
The occurrence of such a local maximum may be identified as the F_1 layer, but since no absolute maximum exists, a theory based solely on recombination- and attachment-type loss mechanisms (Bradbury Theory) cannot provide an adequate explanation of the entire F region of the Earth's ionosphere. When electron-ion diffusion is taken into account, an absolute

maximum is formed in layers governed by attachment-type loss. Since β_{eff} is a decreasing function of altitude, the maximum in the ionization profile does not correspond to the maximum in the production function Q_e , but occurs at a higher altitude.

In the case of the Martian ionosphere, Fjeldbo et al. (1966a) have recently suggested that the probable loss mechanism for electrons is



with a rate coefficient $\beta_3 = 1 \times 10^{-10} \text{ cm}^3/\text{sec.}$ at 300°K (Norton et al., 1966), followed by



with a rate coefficient $\alpha_2 \approx 10^{-7} \text{ cm}^3/\text{sec.}$ at 300°K (Biondi, 1964).

On the basis of these reactions alone, the attachment- and recombination-type loss rates would be

$$4.29) \quad L_a = \beta_3 n_{\text{CO}_2} n_{\text{O}^+} = \beta_{\text{eff}} n_e \quad ; \quad \beta_{\text{eff}} = \beta_3 n_{\text{CO}_2}$$

$$4.30) \quad L_r = \alpha_2 n_{O_2^+} n_e \approx \alpha_2 n_e^2 .$$

These loss rates will be equal at an altitude where

$$4.31) \quad n_e = \frac{\beta_3}{\alpha_2} n_{CO_2} \approx 10^{-3} n_{CO_2} .$$

The ionization maximum in the Martian atmosphere has been observed by Mariner IV at about 125 km. On the basis of a model density distribution in which CO_2 is only ~10% dissociated at 70 km., the CO_2 density at this altitude is about $10^9/cm^3$, the precise value depending on the temperature distribution. Since the observed electron density at the ionization maximum is $\sim 10^5/cm^3$, condition 4.31 will only be satisfied at an altitude well above this maximum. The high CO_2 densities in the Martian atmosphere above the mesopause thus imply that the ionosphere is governed by a recombination-type loss mechanism, i.e., the ionization profile can be described by a Chapman function, and it is not necessary to consider diffusive loss in the Martian ionosphere except at altitudes above the ionization maximum. A further implication of the slight CO_2 dissociation is that the dominant ion in the ionosphere must be O_2^+ rather than O^+ , and the ionization scale height observed by Mariner IV must be

interpreted as implying an exospheric plasma temperature of 200°K rather than 100°K , as would be the case if O^{+} were the dominant ion.

We will assume that the 200°K temperature is characteristic only of the plasma and not of the neutral atmosphere. An elevated daytime plasma temperature has been observed in the F region of the Earth's ionosphere (Brace et al., 1963; Spencer et al., 1965; Sagalyn et al., 1965). (A theoretical treatment of the high electron temperatures in the ionosphere has been carried out by Dalgarno et al. (1963).) The temperature difference results from the high initial energy of the photoelectrons ejected by the solar ultraviolet, which subsequent elastic and inelastic collisions cannot degrade to a value characteristic of the neutral atmosphere. It is likely that such conditions are present in the Martian atmosphere as well.

Mariner IV observed a constant 29 km. plasma scale height extending from just above the ionization maximum to an altitude of about 200 km. For O_2^{+} as the dominant ion in this region (based on an F_1 interpretation), this scale height is characteristic of atomic oxygen at the same temperature as the plasma. If we allow a difference between plasma and neutral temperatures, however, the computed atomic oxygen scale height is

$$4.32) \quad H_O = \frac{T_E}{T_p} H_p ,$$

where $T_p = 200^\circ\text{K}$ and $H_p = 29 \text{ km.}$ are the plasma temperature and scale height, and T_E is the exospheric temperature.

The observed altitude of the ionization maximum in the Martian atmosphere and the constant plasma scale height above this level provide an additional constraint on the computed models. Increasing the heat input increases the computed altitude at which the heating is a maximum. We expect the observed altitude of the ionization maximum to correspond to low effective heating rates. An altitude of 125 km. corresponds to a heat flux of about $.11 \text{ erg/cm}^2\text{sec}$ which is below the value estimated at solar cycle minimum, but within a $\pm 30\%$ uncertainty in the data.

APPENDIX A: DIFFUSION THEORY

The diffusion of neutral constituents in a planetary atmosphere has been discussed by Nicolet and Mange (1954) and by Mange (1957). Specifically, they considered the distribution of chemically active molecular constituents in an atmosphere with linearly varying scale height. Their considerations can be applied to some extent in the present work; in particular, the derivation of the linear terms in the diffusion equation follows Mange (1957).

The mutual diffusion of constituents in a two-component atmosphere is given by Chapman and Cowling (1952) as

$$A.1) \quad \vec{C}_1 - \vec{C}_2 = - \frac{n^2}{n_1 n_2} D_{12} \left[\vec{d}_{12} + \frac{n_T}{T} \vec{\nabla} T \right] .$$

\vec{C}_1 and \vec{C}_2 are the thermal velocities of the constituents, n_1 and n_2 their number densities, n the total density, D_{12} the mutual diffusion coefficient, and n_T is the

thermal diffusion coefficient. \vec{d}_{12} is given by

$$A.2) \quad \vec{d}_{12} = \frac{1}{\rho} (\vec{\nabla} p_1 + \rho_1 \vec{g}) \quad .$$

p_1 and ρ_1 are the partial pressure and mass density of the first gas, and ρ is the total mass density in the case where gravity is the only force acting on the molecules. We write this as

$$A.3) \quad w_1 - w_2 = - \frac{(n_1 + n_2)^2}{n_1 n_2} D_{12} \left\{ \frac{1}{(n_1 + n_2) kT} \left[kT \frac{dn_1}{dz} + n_1 k \frac{dT}{dz} \right] \right. \\ \left. + \frac{n_1 m_1 g}{(n_1 + n_2) kT} + \frac{\kappa_T}{T} \frac{dT}{dz} \right\} \\ = - \frac{n_1 + n_2}{n_2} D_{12} \left\{ \frac{1}{n_1} \frac{dn_1}{dz} + \frac{1}{H_1} + \left[1 + \frac{n_1 + n_2}{n_1} \kappa_T \right] \frac{1}{T} \frac{dT}{dz} \right\} \quad .$$

If the thermal diffusion factor is defined by

$$A.4) \quad \alpha = \frac{(n_1 + n_2)^2}{n_1 n_2} \kappa_T \quad ,$$

the mutual diffusion is given by

$$A.5) \quad w_1 - w_2 = - \frac{n_1 + n_2}{n_2} \left\{ D_{12} \frac{1}{n_1} \frac{dn_1}{dz} + \frac{1}{H_1} + \left[1 + \frac{n_2}{n_1 + n_2} \alpha \right] \frac{1}{T} \frac{dT}{dz} \right\} \quad .$$

In the case of a minor component n_1 diffusing in a stable

main atmosphere, we have $n_1 + n_2 \approx n_2$ and $w_2 = 0$. The diffusion velocity for a minor constituent is thus

$$\text{A.6)} \quad w_1 = -D_{12} \left[\frac{1}{n_1} \frac{dn_1}{dz} + \frac{1}{H_1} + (1 + \alpha) \frac{1}{T} \frac{dT}{dz} \right] .$$

If we assume a linear variation in scale height,

$$\text{A.7)} \quad \frac{1}{T} \frac{dT}{dz} = \frac{1}{H} \frac{dH}{dz} = \frac{\beta}{H}$$

and

$$\text{A.8)} \quad w_1 = -D_{12} \left\{ \frac{1}{n_1} \frac{dn_1}{dz} + \left[\frac{m_1}{m} + (1 + \alpha) \beta \right] \frac{1}{H} \right\} ,$$

the logarithmic derivatives of T and H being equal, since $m_2 \approx m$.

It is on the basis of A.8 that the earlier definition of diffusion time is based. If we take $\frac{d}{dz} \ln T \approx 0$ and $\frac{d}{dz} \ln n \approx 0$, then

$$\text{A.9)} \quad w \approx \frac{D}{H} .$$

The latter condition holds near the maximum of a photochemical distribution, which is where evaluation of the diffusion time τ_D is of greatest interest.

It is convenient to express A.9 in terms of a height

variable ζ introduced by Nicolet (1954) and defined by

$$\text{A.10)} \quad \frac{H}{H_0} = e^{\beta \zeta} \quad .$$

The diffusive velocity is then

$$\text{A.11)} \quad w_1 = - \frac{D_{12}}{H_0} \left[\frac{1}{n_1} \frac{dn_1}{d\zeta} + \frac{m_1}{m} + (1 + \alpha) \beta \right] \quad .$$

We note that in diffusive equilibrium $w_1 = 0$, and the height variation of density is given by

$$\text{A.11a)} \quad n_1 = n_{10} e^{- \left[\frac{m_1}{m} + (1 + \alpha) \beta \right] \zeta} \quad .$$

The continuity equations for the chemical constituents i are, neglecting production and loss terms,

$$\text{A.12)} \quad \frac{\partial n_i}{\partial t} = - \frac{\partial}{\partial z} (n_i w_i) \quad .$$

It is convenient to express these equations in terms of new dependent and independent variables. The new dependent variable u , is defined as the constituent concentration n divided by its diffusion equilibrium altitude variation

$$\text{A.13)} \quad u = n e^{\left[\frac{m_1}{m} + (1 + \alpha) \beta \right] \zeta} \quad .$$

The variation of u thus is a measure of the extent to which the density profile departs from diffusive equilibrium; in diffusive equilibrium $u = \text{constant} = n_0$. The new independent variable y is defined as

$$\text{A.14)} \quad y = e^{\frac{1}{2}(\frac{\beta}{2} - 1) \zeta}.$$

It is virtually certain that in any physical situation of interest $\beta < 2$. For example, in the Martian atmosphere $H \approx (5 \times 10^{-2})T$ km., and a change in scale height $\Delta H/\Delta z$ would require a temperature change of $\Delta T/\Delta z \approx 20 \Delta H/\Delta z$. For $\beta = 2$, we would need a temperature gradient of about 40°K/km. , and atmospheric gradients of this magnitude are not found. As the height variable ζ varies from 0 to ∞ , therefore, y varies from 1 to 0. The variable transformations A.10 and A.14 are not in appropriate form for the case $\beta = 0$, since the relation between z and ζ is then ambiguous. For the isothermal case,* we take $\zeta = z/H$, and hence $y = e^{-z/2H}$. In terms of y we have

*Strictly speaking $\beta = 0$ does not imply $T = \text{constant}$, but rather $H = kT/mg = \text{constant}$. This distinction need not however be emphasized for this discussion.

$$A.15) \quad u = n y^{-2[\gamma + (2 + \beta)/(2 - \beta)]} ,$$

where

$$A.16) \quad \gamma = \frac{m_1/m + \beta\alpha}{1 - \beta/2} - 1 .$$

The diffusion coefficient D is proportional to $\frac{H^{1/2}}{n}$,
where n is the total number density. We thus have

$$A.17) \quad \frac{D/H}{D_o/H_o} = \frac{n_o}{n} \left[\frac{H_o}{H} \right]^{1/2} ,$$

and with

$$A.18) \quad \frac{n_o}{n} = y^{\frac{4(1+\beta)}{\beta-2}}$$

and

$$A.19) \quad \left[\frac{H_o}{H} \right]^{1/2} = y^{-2\beta/(\beta-2)} ,$$

we have

$$A.20) \quad \frac{D}{H} = \frac{D_o}{H_o} y^{2[(\beta+2)/(\beta-2)]} .$$

Using A.20 we find that, in terms of the variables u and y , the diffusive velocity and flux may be written

$$A.21) \quad w_1 = - \frac{\beta - 2}{4} \frac{D_o}{H_o} y^{2(\beta+2)/(\beta-2)} \frac{y}{u} \frac{\partial u}{\partial y}$$

$$A.22) \quad n_1 w_1 = - \frac{\beta - 2}{4} \frac{D_o}{H_o} y^{2\gamma+1} \frac{\partial u}{\partial y} .$$

In terms of these variables, the continuity equation is thus

$$A.23) \quad \frac{1}{\delta^2} \frac{\partial u}{\partial t} = \frac{\partial^2 u}{\partial y^2} + \frac{2\gamma+1}{y} \frac{\partial u}{\partial y} ,$$

where $\delta = \frac{\beta-2}{4} \frac{D_o}{H_o}^{1/2}$. If we now express the time in units of δ^2 so that $\delta^2 t \rightarrow t$, a dimensionless variable, and add the sources and sinks for a given constituent, the continuity equation may be written

$$A.24) \quad \frac{\partial^2 u}{\partial y^2} + \frac{2\gamma+1}{y} \frac{\partial u}{\partial y} - \frac{\partial u}{\partial t} = -Q(u, y) \frac{y^{-2[\gamma+(2+\beta)/(2-\beta)]}}{\delta^2} ,$$

where $Q(u, y)$ is the difference between production and loss terms. With a further change of dependent variable,

$\Omega = y^\gamma u$, A.24 becomes

$$A.25) \quad \frac{1}{y} \frac{\partial}{\partial y} \left[y \frac{\partial \Omega}{\partial y} \right] - \frac{y^2}{y^2} \Omega - \frac{\partial \Omega}{\partial t} = -Q(\Omega, y) \frac{y^{-[\gamma+2(2+\beta)/(2-\beta)]}}{\delta^2} .$$

Solutions of A.24 have been discussed by Mange (1957), for the cases in which Q is either zero or independent of u (or Ω). When this equation is applied to the diffusion of constituents arising in the photolysis of CO_2 , however, the production and loss terms depend on the various number densities and are non-linear as well. The result for the present problem is thus a set of four coupled, non-linear, partial differential equations, and recourse must be made to numerical solution. It is of interest, however, to pursue the formal solution of the continuity equation in the form of A.25, treating Q as independent of Ω . Mange (1957) has taken over directly the solutions of A.25 obtained by Sutton (1943) in regard to another physical problem. (This approach is discussed later.) A method employing Hankel transforms will be used here to solve A.25. It is felt that this method is simpler and more direct than Sutton's somewhat involved boundary-value techniques.

The finite Hankel transform of a function $f(x)$ is defined by

$$\text{A.26) } \quad \bar{f}(p) = \int_0^1 f(x) x J_n(px) dx ,$$

where J_n is a Bessel function of the first kind, of order n ; the method of selecting p is discussed below. The

inversion formula can be represented generally by

$$\text{A.27)} \quad f(x) = \sum_p a_p J_n(px) \quad ,$$

The form of the coefficients a_p depends on the method of selecting p . If p is chosen as a positive root of the equation $J_n(p) = 0$, then an application of the theory of Fourier-Bessel series leads to

$$\text{A.28)} \quad a_p = \frac{2}{J_{n+1}^2(p)} \int_0^1 f(x) x J_n(px) dx = \frac{2\bar{f}(p)}{J_{n+1}^2(p)} \quad ,$$

whereas, if p is taken to be a positive root of the equation

$$\text{A.29)} \quad p J_n'(p) + h J_n(p) = 0 \quad ,$$

where h is a constant, then the appropriate form of a_p is

$$\text{A.30)} \quad a_p = \frac{2p^2 \bar{f}(p)}{h^2 + p^2 - n^2}$$

Generally, the use of an integral transform in solving a partial differential equation temporarily suppresses one of the independent variables, leaving a reduced equation in one less variable. In the case of A.25 above, a finite Hankel transform will be applied to suppress the variable y

(the finite transform being employed because y ranges from 0 to 1).

The physically obvious boundary conditions to use in solving the continuity equation, in any of its forms A.12, A.24, or A.26 are that the diffusive flux be zero at the ground and at the top of the atmosphere, i.e., at $y = 1$ and at $y = 0$. In terms of the variable $u(y)$, A.22 shows that this requirement means

$$\text{A.31)} \quad y^{2\gamma+1} \frac{\partial u}{\partial y} = 0 \quad ,$$

at $y = 1, 0$, or, in terms of the variable $\Omega(y)$,

$$\text{A.32)} \quad y \frac{\partial \Omega}{\partial y} - \gamma \Omega = 0 \quad ,$$

at $y = 1, 0$. Mathematically, it will prove possible to obtain solutions by requiring only that the diffusive flux vanish at the ground

$$\text{A.33)} \quad \frac{\partial \Omega}{\partial y} - \gamma \Omega = 0$$

at $y = 1$, and requiring that $y \partial \Omega / \partial y$ vanish at $y = 0$, the top of the atmosphere. The source term in A.25 will be written $Q(y, t)$, the explicit dependence on Ω being

deleted. It is understood that, in an actual numerical solution, the Ω in Q are evaluated at a previous time step.

The problem of determining the density profiles is now stated as follows: We must solve the equation A.25

$$\frac{1}{y} \frac{\partial}{\partial y} \left[y \frac{\partial \Omega}{\partial y} \right] - \frac{y^2}{y} \Omega - \frac{\partial \Omega}{\partial t} = -Q(y, t) \quad ,$$

subject to the initial condition (the initial density profile)

$$\text{A.34)} \quad \Omega(y, 0) = \Omega_0(y)$$

and to the boundary conditions

$$\text{A.35)} \quad \frac{\partial \Omega}{\partial y} - \gamma \Omega = 0 \quad , \quad y = 1$$

and

$$\text{A.36)} \quad y \frac{\partial \Omega}{\partial y} = 0 \quad , \quad y = 0 \quad .$$

We have for simplicity absorbed the factor $\frac{1}{\delta^2} y^{-(\gamma+2(2+\beta)(2-\beta))}$ into Q .

We multiply A.25 by $y J_\gamma(py)$, where p is chosen,

for reasons which will shortly be apparent, to be a root of

$$A.37) \quad p J_Y'(p) - \gamma J_Y(p) = 0 \quad ,$$

and then we integrate from 0 to 1:

$$\begin{aligned} A.38) \quad & \int_0^1 \frac{\partial}{\partial Y} \left[Y \frac{\partial \Omega}{\partial Y} \right] J_Y(pY) dY - \gamma^2 \int_0^1 \frac{\Omega}{Y} J_Y(pY) dY \\ &= Y \frac{\partial \Omega}{\partial Y} J_Y(pY) \Big|_0^1 - p \int_0^1 Y \frac{\partial \Omega}{\partial Y} J_Y'(pY) dY - \gamma^2 \int_0^1 \frac{\Omega}{Y} J_Y(pY) dY \\ &= \frac{\partial \Omega}{\partial Y} J_Y(p) \Big|_{Y=1} - p \left[Y \Omega J_Y'(pY) \right]_0^1 \\ &\quad + p \int_0^1 \Omega \left[\frac{\partial}{\partial Y} (Y J_Y'(pY)) - \frac{Y^2}{pY} J_Y(pY) \right] dY \quad . \end{aligned}$$

Integration by parts has been used in these steps, and A.37 has been used in the second step. Combining terms and carrying out the differentiation under the integral sign, we have, for the first two terms of A.25

$$\begin{aligned} A.39) \quad & \left[\frac{\partial \Omega}{\partial Y} J_Y(p) - p \Omega J_Y'(p) \right]_{Y=1} \\ &+ p \int_0^1 \Omega \left[pY J_Y''(pY) + J_Y'(pY) - \frac{Y^2}{pY} J_Y(pY) \right] dY \quad . \end{aligned}$$

Due to the choice A.37 of p , and to the boundary condition

A.35, the first term is

$$A.40) \quad J_Y(p) \left[\frac{\partial \Omega}{\partial Y} - \gamma \Omega \right]_{Y=1} = 0 \quad .$$

Since $J_Y(pY)$ satisfies Bessel's equation

$$A.41) \quad J_Y''(pY) + \frac{1}{pY} J_Y'(pY) + \left[1 - \frac{Y^2}{2Y^2} \right] J_Y(pY) = 0 \quad ,$$

the integral is just

$$A.42) \quad -p^2 \int_0^1 \Omega_Y J_Y(pY) dY = -p^2 \bar{\Omega}(p, t) \quad .$$

The finite Hankel transform of A.25 is thus

$$A.43) \quad \frac{d\bar{\Omega}}{dt} + p^2 \bar{\Omega} = \bar{Q} \quad ,$$

where

$$A.44) \quad \bar{Q}(p, t) = \int_0^1 Q(Y, t) Y J_Y(pY) dY \quad .$$

Since p is a root of A.37, the appropriate inversion formula is given by A.30 with $h = n$, and hence

$$A.45) \quad \Omega(Y, t) = 2 \sum_p \bar{\Omega}(p, t) \frac{J_Y(pY)}{J_Y^2(p)} \quad .$$

The solution of A.43 is

$$A.46) \quad \bar{\Omega}(p, t) = \bar{\Omega}_0(p) e^{-p^2 t} + \int_0^t dt' e^{-p^2(t-t')} \bar{Q}(p, t') ,$$

where

$$A.47) \quad \bar{\Omega}_0(p) = \int_0^1 dy' y' J_Y(pY') \Omega_0(y')$$

and

$$A.48) \quad \bar{Q}(p, t') = \int_0^1 dy' y' J_Y(pY') Q(y', t') .$$

Hence,

$$A.49) \quad \bar{\Omega}(p, t) = e^{-p^2 t} \int_0^1 dy' y' J_Y(pY') \Omega_0(y') \\ + \int_0^t dt' e^{-p^2(t-t')} \int_0^1 dy' y' J_Y(pY') Q(y', t') .$$

Using the inversion formula A.45 the solution becomes

$$A.50) \quad \Omega(y, t) = \int_0^1 G_1(y, y'; t) y' \Omega_0(y') dy' \\ + \int_0^t dt' \int_0^1 G_2(y, y'; t, t') y' Q(y', t') dy' ,$$

where

$$A.51) \quad G_1(y, y'; t) = 2 \sum_{p>0} e^{-p^2 t} \frac{J_Y(py) J_Y(py')}{J_Y^2(p)}$$

and

$$A.52) \quad G_2(y, y'; t, t') = 2 \sum_{p>0} e^{-p^2(t-t')} \frac{J_Y(py) J_Y(py')}{J_Y^2(p)}.$$

From the definition A.13 of u and the relation $\Omega = y^Y u$, we have the relation between the density variables n and Ω .

$$A.53) \quad n(y, t) = y^{Y+2(2+\beta)/(2-\beta)} \Omega(y, t).$$

The solution A.50 in terms of n becomes

$$A.54) \quad n(y, t) = y^{\left[Y+2 \frac{2+\beta}{2-\beta} \right]} \int_0^1 y'^{\left[\frac{3\beta+2}{\beta-2} - Y \right]} G_1(y, y'; t) n_0(y') dy' \\ + y^{\left[Y+2 \frac{2+\beta}{2-\beta} \right]} \int_0^t dt' \int_0^1 G_2(y, y'; t, t') y' Q(y', t') dy'.$$

We can see from A.54 that the density profile approaches a diffusive distribution at high altitudes as would be expected. As $y \rightarrow 0$ the Bessel function in G_1 or G_2 , having a y -dependent argument, behaves as y^Y , and, thus, $n(y)$ behaves as $y^{2(Y+1)} = e^{-z/H'}$, where $H' = \frac{\bar{m}}{m} \bar{H}$ is

the scale height for a constituent of mass m' , and we have taken $\beta = 0$ for simplicity.

A Comment on Mange's Solution

As previously noted, Mange (1957) has presented a solution of A.25. Reference to his equation 5.1 or 6.9 shows that it is not of the same form as A.54. Instead of integrals over the functions G_1 and G_2 of A.54, which are themselves a sum of products of Bessel functions of the first kind, Mange's solution contains an integral over a Bessel function of imaginary argument of the first kind, $I_\gamma(y)$. This difference is due to the fact that Mange uses the solution of the sourceless form of A.25 obtained by Sutton (1943).

Sutton's equation, though identical in form with A.25, contains an independent variable with a range from 0 to ∞ rather than from 0 to 1. This difference in the range of the independent variable necessitates the application of boundary conditions at different points, which in turn results in different solutions. Mange's solution, then, is appropriate only for an atmosphere which extends infinitely downward so that as $z \rightarrow \infty$, $y \rightarrow \infty$. Such a solution would be useful if there were no transport to ground level of any of the constituents being considered.

The solution of A.25 for the infinite atmosphere can be obtained by a procedure analogous to that used in deriving A.50 and A.54. In this case the (infinite) Hankel transform may be employed. The Hankel transform pair for the dependent variable Ω of A.25 is

$$\text{A.55) } \Omega(y, t) = \int_0^\infty \bar{\Omega}(\xi, t) \xi J_\gamma(y\xi) d\xi$$

and

$$\text{A.56) } \bar{\Omega}(\xi, t) = \int_0^\infty \Omega(y, t) y J_\gamma(\xi y) dy .$$

Multiplying A.25 by $y J_\gamma(\xi y)$ and integrating from 0 to ∞ , we obtain for the transform of the first two terms

$$\begin{aligned} \text{A.57) } & y \left[J_\gamma(\xi y) \frac{\partial \Omega}{\partial y} - \xi J_\gamma'(\xi y) \Omega \right] \Big|_{y=0}^{y=\infty} \\ & + \xi \int_0^\infty \Omega \left[\xi y J_\gamma'' + J_\gamma' - \frac{y^2}{\xi y} J_\gamma \right] dy . \end{aligned}$$

The first term of A.57 may be written

$$\text{A.58) } \left\{ J_\gamma(\xi y) \left[y \frac{\partial \Omega}{\partial y} - \gamma \Omega \right] + \xi y J_{\gamma+1}(\xi y) \Omega \right\} \Big|_{y=0}^{y=\infty} .$$

This vanishes at $y = 0$, but the situation at $y = \infty$ is

somewhat more complicated.

According to Mange, useful solutions can be obtained for the condition that the diffusive flux vanish as $y \rightarrow \infty$; however, in this circumstance only the term in square brackets above will vanish. As $y \rightarrow \infty$, we have $\xi y J_{\gamma+1}(\xi y) \rightarrow (\xi y)^{1/2}$. In order for the second term to vanish, we require $\Omega(y) \approx y^c$ with $c < -1/2$ as $y \rightarrow \infty$. In diffusive equilibrium $\Omega(y)$ goes as y^γ , and we may say that our constituent approaches diffusive equilibrium as $y \rightarrow \infty$ only if the γ of A.16, i.e., not the absolute value, is less than $-1/2$. For an isothermal atmosphere this could mean $m_1/\bar{m} < 1/2$, and we could obtain solutions satisfying the requirement of diffusive equilibrium only for constituents whose mass is less than half the mean atmospheric mass. For $\beta > 0$ the mass requirement is even more stringent.

Physically, however, it would seem that there is no need to impose such restrictive mass requirements, i.e., we need not require diffusive equilibrium. In most instances we will be interested in the density profiles of constituents which are removed from low altitudes by chemical processes, and in such cases a low altitude diffusive equilibrium requirement would be physically incorrect. Even in the absence of a removal mechanism, downward diffusion will become ever more

difficult as the mean atmospheric density increases,
 $\tau_D \approx H^2/D \rightarrow \infty$ ($D \rightarrow 0$) , and diffusive equilibrium is unlikely.
 In the absence of a removal mechanism, of course, a constituent will be transported to the ground and the density distribution for such a constituent could not be obtained by these methods.

In view of these arguments, we simply suppose that the first term of A.57 vanishes, i.e., that $\Omega \approx y^c$ as $y \rightarrow \infty$ ($c < -1/2$) , and that this imposes no restriction on γ .
 The consistency of this argument may be checked once a solution is obtained.

The Hankel transform of A.25 has the same form as A.43

$$\text{A.59) } \frac{d\bar{\Omega}}{dt} + \xi^2 \bar{\Omega} = \bar{Q}(\xi, t) \quad ,$$

and as before

$$\text{A.60) } \bar{\Omega}(\xi, t) = \bar{\Omega}_0(\xi) e^{-\xi^2 t} + \int_0^t \bar{Q}(\xi, t') e^{-\xi^2(t-t')} dt' \quad .$$

With the aid of A.55 and A.56, A.60 becomes

$$\begin{aligned} \text{A.61) } \Omega(y, t) = & \int_0^\infty \Omega_0(y') \mathcal{L}_1(y, y'; t) dy' \\ & + \int_0^t dt' \int_0^\infty dy' y' \mathcal{L}_2(y, y'; t, t') Q(y', t') \quad , \end{aligned}$$

where (Watson, 1944, Chapter 13)

$$\begin{aligned} \text{A.62) } \mathcal{L}_1(y, y'; t) &= \int_0^\infty e^{-t\xi^2} \xi J_Y(y\xi) J_Y(y'\xi) d\xi \\ &= \frac{1}{2t} e^{-(y^2 + y'^2)/4t} I_Y\left[\frac{yy'}{2t}\right] \end{aligned}$$

and

$$\begin{aligned} \text{A.63) } \mathcal{L}_2(y, y'; t, t') &= \int_0^\infty e^{-(t-t')\xi^2} \xi J_Y(y\xi) J_Y(y'\xi) d\xi \\ &= \frac{1}{2(t-t')} e^{-(y^2 + y'^2)/4(t-t')} I_Y\left[\frac{yy'}{2(t-t')}\right]. \end{aligned}$$

I_Y is the Bessel function of the first kind, of imaginary argument. Using A.62 and A.63 the solution for Ω becomes

$$\begin{aligned} \text{A.64) } \Omega(y, t) &= \frac{e^{-\frac{y^2}{4t}}}{2t} \int_0^\infty w e^{-\frac{w^2}{4t}} I_Y\left[\frac{yw}{2t}\right] \Omega_0(w) dw \\ &+ \int_0^t dt' \frac{e^{-\frac{y^2}{4(t-t')}}}{2(t-t')} \int_0^\infty w e^{-\frac{w^2}{4(t-t')}} I_Y\left[\frac{yw}{2(t-t')}\right] Q(w, t') dw. \end{aligned}$$

The first term of A.64 corresponds to Mange's presentation of Sutton's solution of the sourceless form of A.25 (Mange's equation 5.1), and the second term corresponds to Mange's equation 6.9, which he derived heuristically. If the

dimensionless variable t in A.64 is replaced by t^2 and the transformation A.53 between n and Ω is used, these terms become identical with those in Mange's paper.

Due to the analytic form of the Green's functions for the case of the infinite atmosphere, the use of A.64 is to be preferred over the solution A.53 for the semi-infinite atmosphere when such use is physically justifiable.

Steady State Solutions

The steady-state solutions of A.25 are readily obtained by deleting the time derivative from the transformed equations A.43 and A.59. The density profiles are found to be

$$A.65) \quad \Omega(y) = \int_0^1 G_s(y, y') y' Q(y') dy'$$

with

$$A.66) \quad G_s(y, y') = 2 \sum_{p>0} \frac{J_y(py) J_y(py')}{p^2 J_y^2(p)}$$

for the semi-infinite case, and

$$A.67) \quad \Omega(y) = \int_0^\infty \mathcal{G}_s(y, y') y' Q(y') dy'$$

with

$$\text{A.68) } \mathcal{L}_s(y, y') = \int_0^\infty \frac{J_\gamma(y\xi) J_\gamma(y'\xi)}{\xi} d\xi$$

for the infinite case. According to Watson (1944, p. 405) the function $\mathcal{L}_s(y, y')$ of A.68 has the following form

$$\begin{aligned} \mathcal{L}_s(y, y') &= \frac{1}{2\gamma} \left[\frac{y'}{y} \right]^\gamma & y' < y \\ \text{A.69) } \mathcal{L}_s(y, y') &= \frac{1}{2\gamma} \left[\frac{y}{y'} \right]^\gamma & y' > y \end{aligned}$$

for $\text{Re}(\gamma) > 0$. The steady-state solution of the diffusion equation for the infinite atmosphere thus takes the relatively simple form

$$\text{A.70) } \Omega(y) = \frac{1}{2\gamma y^\gamma} \int_0^y y'^{\gamma+1} Q(y') dy' + \frac{y^\gamma}{2\gamma} \int_y^\infty y'^{1-\gamma} Q(y') dy' ,$$

provided $\gamma > 0$, i.e., the constituent under discussion is heavier than the mean atmospheric mass. For $\gamma < 0$ there appears to be an unavoidable singularity in \mathcal{L}_s , and the solution fails in this case. The steady-state diffusion problem can still be solved, but the equation A.65 for the semi-infinite atmosphere must be used.

APPENDIX B: VIBRATIONAL EXCITATION

Collisional excitation of the vibrational states of a harmonic oscillator was first thoroughly treated by Jackson and Mott (1932), who considered the one-dimensional collision of a diatomic molecule with an atom and developed the distorted-wave solution of the Schrodinger equation. Their treatment was extended to the collision of two diatomic molecules by Takayanagi (1952), and to the three-dimensional case by Schwartz and Herzfeld (1954).

The solution of the problem given below differs from that of these authors chiefly in the adoption of the scattering matrix point of view, as developed by Blatt and Biedenharn (1952) and employed by Arthurs and Dalgarno (1960) and by Davison (1961) in connection with their treatment of rotational transitions. It is hoped that some uniformity of approach to the overall problem of collisional excitation might be engendered by exhibiting the relevance of this

method to vibrational transitions.

The computation will be carried through with reference to vibrational excitation of the CO molecule.

The vibrational cooling term may be written as

$$B.1) \quad R_v(CO|z, T) = n_M(z)n(CO|z)\eta_{12}(T)h\nu \quad ,$$

where $n_M(z)$ is the number density of molecules with which the CO molecules may collide. The vibrational activation coefficient is related to the collision cross section σ_{12} by

$$B.2) \quad \eta_{12}(T) = \langle \sigma_{12}(w)w \rangle \quad ,$$

where w is the molecular velocity and the brackets represent an averaging over the Maxwellian velocity distribution.

The first step will be to derive an expression for σ_{12} in terms of the scattering matrix, to be defined below. The form of the intermolecular potential which appears in this expression will then be discussed, and finally the scattering matrix and σ_{12} will be evaluated and the latter averaged according to B.2 to obtain η_{12} .

The coordinates describing the collision will be taken as r , the separation of the centers of mass of the collid-

ing molecules, θ , the scattering angle, and ξ_1 , ξ_2 , the vibrational coordinates of the molecules. We wish to describe the scattering of a plane wave, carrying the initial states, from a scattering center and will define the scattering matrix in terms of the asymptotic form of the wave function after the scattering.

The Hamiltonian of the system is the sum of the translational and vibrational energy operators plus the interaction potential

$$\text{B.3)} \quad H = -\frac{\hbar^2}{2\mu} \nabla_{\vec{r}}^2 + H_{v_1} + H_{v_2} + V(\vec{r}, \xi_1, \xi_2) \quad ,$$

where μ is the reduced mass of the colliding molecules.

The vibrational Hamiltonians are

$$\text{B.4)} \quad H_{v_1} = -\frac{\hbar^2}{2\mu_1} \nabla_{\xi_1}^2 + 2\pi^2 \mu_1^2 \xi_1^2 \quad ,$$

with a similar form for H_{v_2} . ν_1 is the molecular vibration frequency. The subscript on the operator ∇ indicates the coordinate on which it operates. The wave function $\Psi(\vec{r}, \xi_1, \xi_2)$ satisfies the equation

$$\text{B.5)} \quad (H - \mathcal{E})\Psi = 0 \quad ,$$

where \mathcal{E} , the total energy of the system, is given by

$$\text{B.6) } \mathcal{E} = \frac{\hbar^2 k_n^2}{2\mu} + (n_1 + \frac{1}{2})h\nu_1 + (n_2 + \frac{1}{2})h\nu_2 \quad .$$

n_1 and n_2 are vibrational quantum numbers, and k_n is the wave number of the system, these being the values before collision. The complete wave function for the system will be written

$$\text{B.7) } \Psi(r, \theta, \xi_1, \xi_2) = \sum_{l=0}^{\infty} \sum_{n'_1 n'_2} A_{n'}^l \frac{u_{nn'}^l(r)}{r} y_{l,0}(\theta) h_{n'_1}(\xi_1) h_{n'_2}(\xi_2) \quad .$$

This is the partial wave expansion of Ψ . The radial wave functions are denoted by $u_{nn'}^l$, where the single subscripts n and n' stand for the pairs of vibrational quantum numbers n_1, n_2 and n'_1, n'_2 , primes denoting the values after collision. The $h_{n'_1}$ and $h_{n'_2}$ are harmonic oscillator wave functions, $y_{l,0}$ is a spherical harmonic, and $A_{n'}^l$ are constants to be determined. The sum is over all values of n_1 and n_2 , before and after collision. The incident wave is

$$\begin{aligned} \text{B.8) } \Psi_{\text{in}} &= h_{n_1} h_{n_2} e^{ik_n z} \\ &= h_{n_1} h_{n_2} \sum_{l=0}^{\infty} (2l+1) i^l j_l(kr) P_l(\cos \theta) \quad , \end{aligned}$$

and the asymptotic form is, writing

$$\text{B.9)} \quad y_{\ell,0} = \left[\frac{2\ell+1}{4\pi} \right]^{\frac{1}{2}} P_{\ell}(\cos \theta) \quad ,$$

$$\text{B.10)} \quad \psi_{in} = h_{n_1} h_{n_2} \frac{\pi^{\frac{1}{2}}}{k_n r} \sum_{\ell} (2\ell+1)^{\frac{1}{2}} i^{(\ell+1)} \left[e^{-i(k_n r - \frac{\ell\pi}{2})} - e^{i(k_n r - \frac{\ell\pi}{2})} \right] y_{\ell,0} \quad .$$

Asymptotically, the radial function $u_{nn'}^{\ell}(r)$ must therefore consist of an incoming spherical wave and elastically scattered outgoing spherical wave in the entrance channel and an inelastically scattered outgoing spherical wave in the exit channel. The terms "entrance" and "exit" channel are used, as in Blatt and Biedenharn (1952), to denote sets of quantum numbers which specify the configuration of the system before and after collision. We thus write the asymptotic form of $u_{nn'}^{\ell}$ as

$$\text{B.11)} \quad u_{nn'}^{\ell}(r) = \delta_{nn'} e^{-i(k_n r - \frac{\ell\pi}{2})} - \left[\frac{k_n}{k_{n'}} \right]^{\frac{1}{2}} S^{\ell}(n,n') e^{i(k_{n'} r - \frac{\ell\pi}{2})} \quad .$$

This is the definition of the scattering matrix $S^{\ell}(n,n')$

used by Arthurs and Dalgarno (1960). To obtain the scattered wave, the incident wave B.10 is subtracted from B.7. The summation in B.10 may be extended to a sum over n' if the right hand side is first multiplied by $\delta_{nn'}$. The terms multiplying $e^{-i(k_n r - \frac{l\pi}{2})}$ and $e^{i(k_n r - \frac{l\pi}{2})}$ in the expression for the scattered wave function may then be combined, and the condition that there be no ingoing scattered spherical wave determines the coefficients $A_{n'}^l$. The results for $A_{n'}^l$ and the scattered wave are

$$\text{B.12)} \quad A_{n'}^l = \frac{\pi^{\frac{1}{2}}}{k_{n'}} (2l+1)^{\frac{1}{2}} i^{l+1}$$

$$\begin{aligned} \text{B.13)} \quad \psi_{sc} = & \sum_l \sum_{n'} \left[\frac{\pi}{k_n k_{n'}} \right] (2l+1)^{\frac{1}{2}} i^{l+1} T^l(n, n') \\ & \times \frac{e^{i(k_n r - \frac{l\pi}{2})}}{r} y_{l,0} h_{n'_1} h_{n'_2} \end{aligned}$$

where

$$\text{B.14)} \quad T^l(n, n') = \delta_{nn'} - S^l(n, n') .$$

The total scattering cross section is given by the number of particles scattered per unit time divided by the incident flux. The number scattered per unit time is

$$\text{B.15)} \quad N_{sc} = - \frac{i\hbar}{2\mu} \int (\psi_{sc}^* \nabla \psi_{sc} - \psi_{sc} \nabla \psi_{sc}^*) r_o^2 d\Omega ,$$

where r_o is the radius of a sphere centered on and distant from the scattering center and $d\Omega$ is the element of solid angle. Using the ψ_{sc} of B.13 in B.15 results in

$$\text{B.16)} \quad N_{sc} = \frac{\hbar k_{n'}}{2\mu} \frac{\pi}{k_n k_{n'}} \sum_{l=0}^{\infty} (2l+1) |T^l(n, n')|^2 ,$$

and dividing by the incident flux $\hbar k_n / 2\mu$ we obtain the total cross section

$$\text{B.17)} \quad \sigma(n, n') = \pi \lambda_n^2 \sum_{l=0}^{\infty} (2l+1) |T^l(n, n')|^2 ,$$

where $\lambda_n = 1/k_n$. We are interested in the cross section for a specific transition in which the final state n' is specified and so the sum over n' in B.13 has been dropped.

Knowledge of the scattering matrix must be obtained by solving the Schrodinger equation appropriate to the system.

If B.7 is substituted in B.6, the result multiplied by

$y_{l'0}^h y_{n_1''}^h y_{n_2''}^h$ and integrated over $d\xi_1 d\xi_2 d\Omega$, we obtain the equation for the radial functions $u_{nn'}^l(r)$

$$\text{B.18)} \quad \left[\frac{d^2}{dr^2} - \frac{l(l+1)}{r^2} + k_{n''}^2 \right] u_{nn''}^l = \frac{2\mu}{\hbar^2} \sum_{n'} \langle n'' | V | n' \rangle u_{nn'}^l,$$

where

$$\text{B.19)} \quad \langle n'' | V | n' \rangle = \iint h_{n''_1}(\xi_1) h_{n''_2}(\xi_2) V(\vec{r}, \xi_1, \xi_2) h_{n'_1}(\xi_1) h_{n'_2}(\xi_2) d\xi_1 d\xi_2.$$

Equations B.18 are the exact equations for the radial functions $u_{nn''}^l$, but they cannot be solved in general in terms of known functions. Before discussing approximations which render a solution of B.18 possible, we will discuss the form of the intermolecular potential appearing in these equations.

It is customary to divide intermolecular forces into two types: long-range, attractive (van der Waals) forces, and short-range, repulsive (valence or chemical) forces. The long-range forces can be rigorously described in terms of physical properties of the separated molecules, but no such general treatment exists for the short-range forces. The usual practice is to adopt a semi-empirical potential function for use in calculations, the parameters upon which this function depends being determined from measured physical properties. It can be argued that transition probabilities in collision depend essentially on the short-range, repulsive forces rather than the long-range forces, and for this reason

earlier investigators assumed a simple exponential interaction law for mathematical convenience. The long-range forces do, however, have the effect of accelerating the colliding molecules before the short-range forces come into play and will thus affect the temperature dependence of physical quantities, such as the vibrational deactivation coefficient, calculated using the potential function. For this reason, it is desirable to take the van der Waals forces into explicit account.

One of the most commonly used potential functions is that of Lennard-Jones

$$\text{B.20)} \quad V(r) = 4\epsilon \left\{ \left[\frac{r_0}{r} \right]^{12} - \left[\frac{r_0}{r} \right]^6 \right\} .$$

The negative term represents the attraction, the sixth power being the theoretically calculated form of this interaction. The twelfth power form of the much steeper repulsive potential is chosen for mathematical convenience. The form of this function is sketched in Fig. B1. ϵ is the minimum value of V , and r_0 is the distance at which $V = 0$. The effect of the repulsive part of the potential may be retained, and the convenience of an exponential form utilized by fitting an exponential curve to the Lennard-Jones potential.

Methods of fitting an exponential to the Lennard-Jones

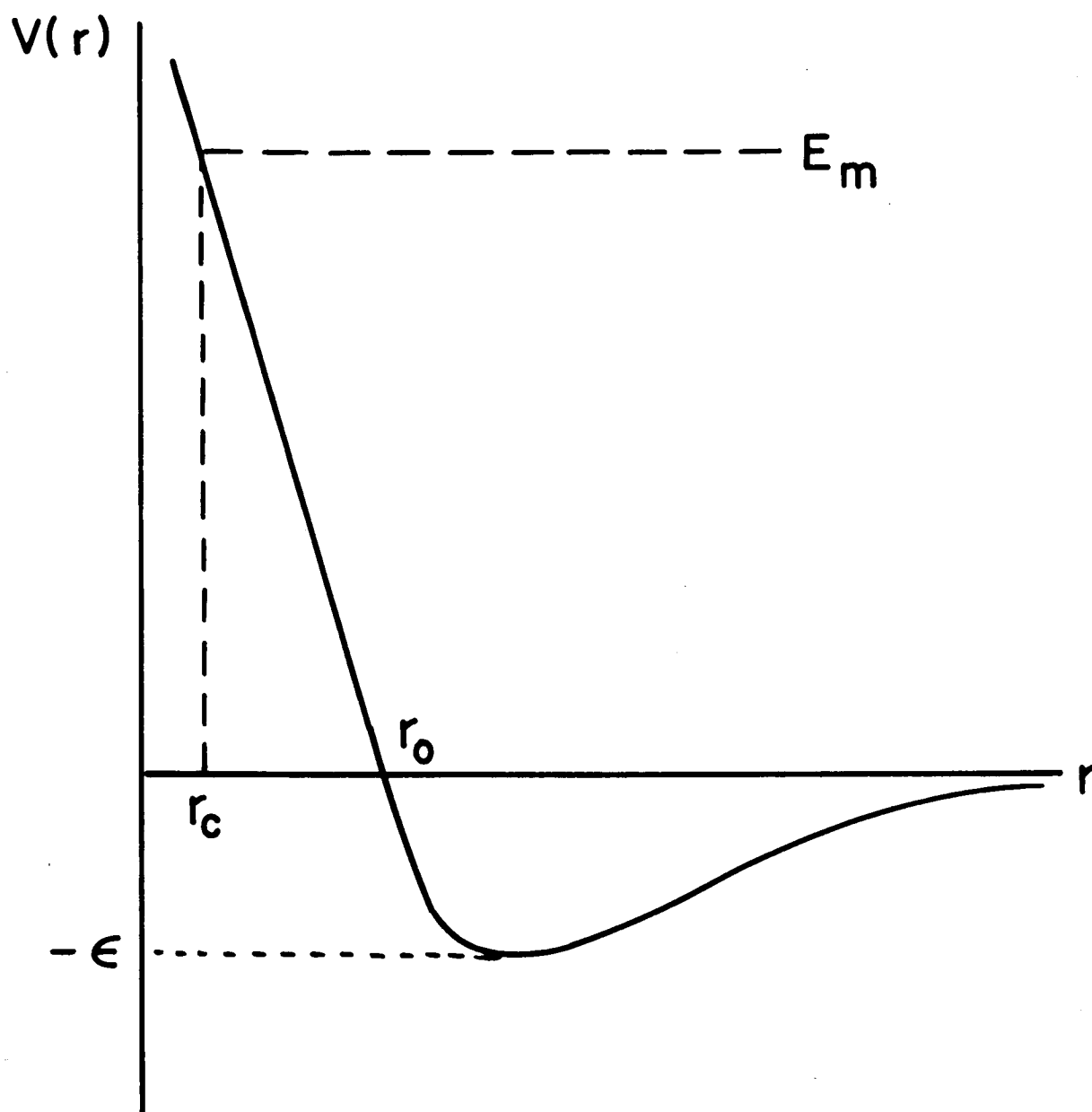


Fig. B1. Lennard-Jones potential curve. E_m is the most effective energy of collision at the classical distance of closest approach r_c .

curve were devised by Schwartz et al. (1952) and by DeWette and Slawsky (1954) and discussed by Herzfeld and Litovitz (1959). In the method of Schwartz et al., the two curves are required to have the same slope at a common point, whereas DeWette and Slawsky obtain a fit by having two points in common. This latter method is somewhat simpler and will be employed. Both methods lead to results in reasonable agreement with experimental measurement of relaxation times.

In both methods one point of fitting is that for the most effective energy of collision E_m at the classical distance of closest approach r_c . The energy E_m is defined by $E_m = \frac{1}{2} m w_m^2$ where w_m is the velocity at which, classically, a vibrational transition is most likely to occur. This velocity exists due to the fact that the probability of energy transfer in collision increases with increasing velocity, but the number of particles with a given velocity decreases. Hence, at some value of w the probability of energy transfer is a maximum. Herzfeld and Litovitz show that E_m is given by

$$\text{B.21)} \quad E_m = \frac{1}{2} (\epsilon')^{1/3} (kT)^{2/3} ,$$

where

$$\text{B.22)} \quad \epsilon' = \mu_m (2\pi\nu\ell')^2 .$$

μ_m is the reduced mass of the diatomic molecule, ν its vibrational frequency, and ℓ' a characteristic length. ϵ' is twice the energy a molecule would have if it were vibrating with amplitude ℓ' and frequency ν . r_o and ϵ are given for various gases by Hirschfelder, Curtiss, and Bird (1954), and r_c is calculated from

$$\text{B.23)} \quad E_m = 4\epsilon \left\{ \left[\frac{r_o}{r_c} \right]^{12} - \left[\frac{r_o}{r_c} \right]^6 \right\}$$

or

$$\text{B.24)} \quad \frac{r_o}{r_c} = \left\{ \frac{1}{2} \left[1 + \sqrt{\frac{E_m}{\epsilon} + 1} \right] \right\}^{1/6} .$$

Since the Lennard-Jones curve has a minimum at $-\epsilon$, the exponential which can be substituted for this potential along its sweep part must have its horizontal asymptote at $V = -\epsilon$. The exponential curve

$$\text{B.25)} \quad V(r) = V_o e^{-r/L} - \epsilon$$

satisfies this requirement and contains two constants, V_o

and L , to be determined so that it crosses the Lennard-Jones curve at two points. To fit the curves at the point mentioned above we have

$$\text{B.26)} \quad E_m + \epsilon = V_o e^{-r_c/L}.$$

If we also require the point $E = 0$, $r = r_o$ to be common, then

$$\text{B.27)} \quad V_o e^{-r_o/L} - \epsilon = 0.$$

Dividing B.24 by B.25, and solving for r_o/L results in

$$\text{B.28)} \quad \frac{r_o}{L} = \ln \left[\frac{E_m}{\epsilon} + 1 \right] \left\{ 1 - \left[\frac{1}{2} \left(1 + \sqrt{\frac{E_m}{\epsilon} + 1} \right) \right]^{-1/6} \right\}.$$

In practice L is obtained first from B.28 and then V_o from B.27. An equation such as B.25 represents the potential between two atoms, r being their separation. In describing molecular collisions this potential must be stated in terms of coordinates referring to the molecules. A method of evaluating the intermolecular potential has been given by Takayanagi (1954). The repulsive part of the intermolecular potential may be expressed approximately by the sum of the interatomic repulsive potentials between atoms belonging to

different molecules. With reference to Fig. B2 we write

$$\text{B.29) } V_r = V_{13}(r_{13}) + V_{14}(r_{14}) + V_{23}(r_{23}) + V_{24}(r_{24}) ,$$

where r_{ij} is the distance between the i^{th} and j^{th} atoms.

Denote the internuclear distances in the molecules by ξ_1 and ξ_2 and the distance between the centers of mass by R .

If the internuclear distances are both small compared with the intermolecular distance R , the function B.29 can be expanded as

$$\begin{aligned} \text{B.30) } V_r = & \sum_{a=1,2} \sum_{b=3,4} \sum_{ijklmn} \frac{x_a^i y_a^j z_a^k}{i!j!k!} \frac{x_b'^l y_b'^m z_b'^n}{l!m!n!} \\ & \times \left[\frac{\partial^{i+j+k+l+m+n} V_{ab}(r)}{\partial x^i \partial y^j \partial z^k \partial x'^l \partial y'^m \partial z'^n} \right]_{\substack{x=y=z=0 \\ x'=y'=z'=0}} \end{aligned}$$

where

$$\text{B.31) } r^2 = (x' - x - R)^2 + (y' - y)^2 + (z' - z)^2 .$$

It is convenient, after writing out a few terms of B.30 in Cartesian coordinates, to transform V_r to a function of $\cos \chi_1$, $\cos \chi_2$, and $\cos \chi_{12}$, where χ_{12} is the angle between the unit vectors $\hat{\xi}_1$, $\hat{\xi}_2$ along the molecular axes.

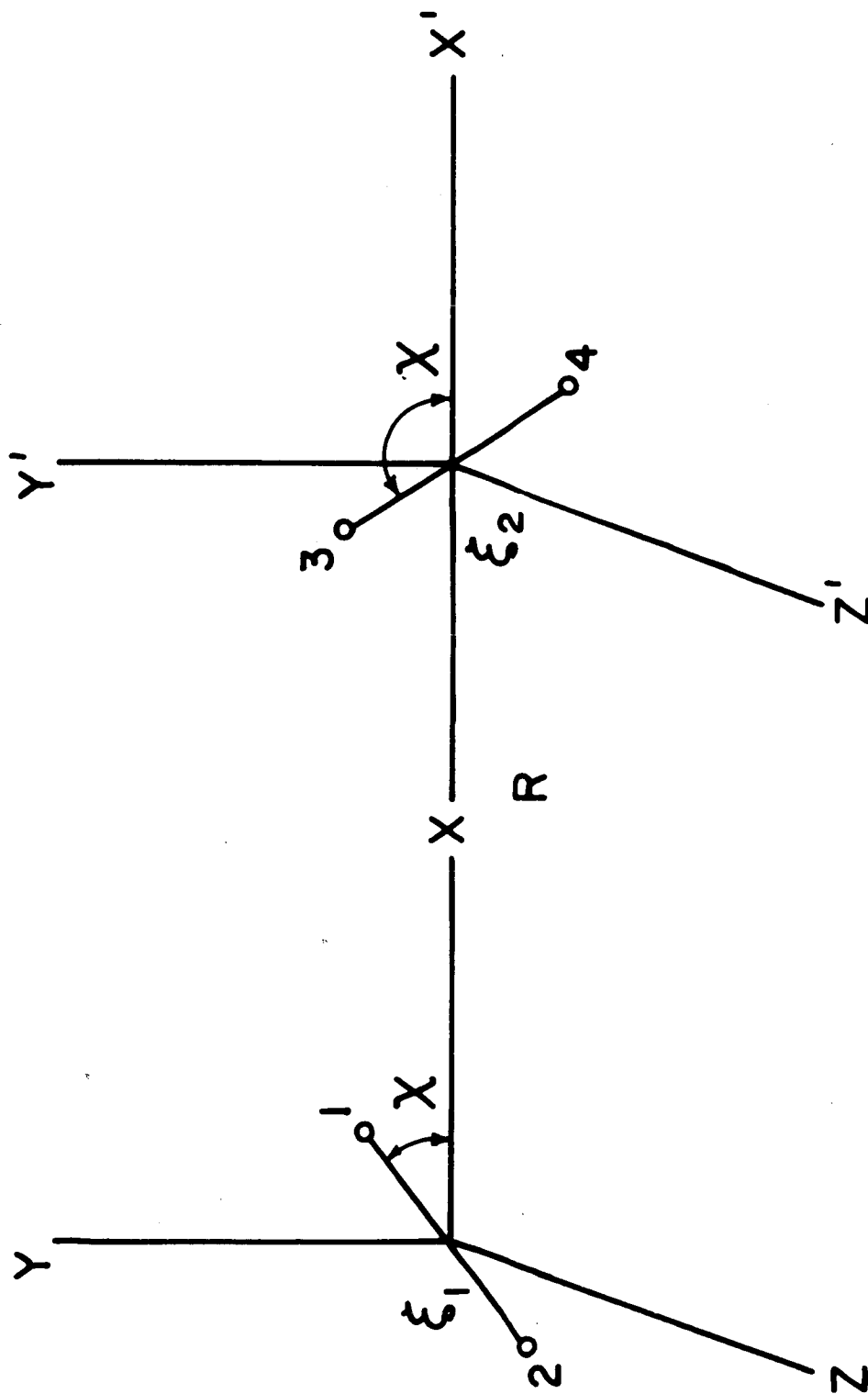


Fig. B2. Coordinates used in evaluation of the intermolecular potential.

The transformation formulae are

$$x_1 = \frac{m_1}{m_{12}} \xi_1 \cos \chi_1$$

$$\text{B.32)} \quad y_1^2 + z_1^2 = \left[\frac{m_1}{m_{12}} \right]^2 \xi_1^2 (1 - \cos^2 \chi_1)$$

$$y_1 y_3 + z_1 z_3 = \frac{m_2 m_4}{m_{12} m_{34}} \xi_1 \xi_2 (\cos \chi_{12} - \cos \chi_1 \cos \chi_2) \quad .$$

The term ϵ in B.25 may be absorbed in k^2 when $V(r)$ appears in the Schrodinger equation, i.e., k^2 is replaced by $k^2 + 2\mu\epsilon/\hbar^2$. The interatomic potential terms in B.29 may thus be taken to have the form

$$\text{B.33)} \quad V(r) = V'_0 e^{-r/L} \quad .$$

The result of carrying the expansion of V to second order is

$$\begin{aligned} \text{B.34)} \quad V(R, \xi_1, \xi_2) = & 4V'_0 e^{-R/L} + \frac{2V'_0}{L} \left[\frac{m_1 - m_2}{m_{12}} \xi_1 \cos \chi_1 - \frac{m_3 - m_4}{m_{34}} \xi_2 \cos \chi_2 \right] e^{-R/L} \\ & + \frac{V'_0}{L^2} \left\{ \frac{m_1^2 + m_2^2}{m_{12}} \xi_1^2 \left[\cos^2 \chi_1 + \frac{L}{R} (1 - \cos^2 \chi_1) \right] + \frac{m_3^2 + m_4^2}{m_{34}} \xi_2^2 \left[\cos^2 \chi_2 + \frac{L}{R} (1 - \cos^2 \chi_2) \right] \right. \\ & \left. - \frac{(m_1 - m_2)(m_3 - m_4)}{m_{12} m_{34}} \xi_1 \xi_2 \left[\cos \chi_1 \cos \chi_2 + \frac{L}{R} (\cos \chi_{12} - \cos \chi_1 \cos \chi_2) \right] \right\} e^{-R/L} \quad . \end{aligned}$$

Only the first term in this expansion contributes to the diagonal matrix elements in B.18. For a collision such as that of a CO molecule with a structureless particle, i.e., with a molecule whose internal coordinates are unaltered by collision, only the term in $\xi_1 \cos \chi_1$ contributes to the off-diagonal elements. Higher order terms in B.34 give rise to matrix elements connecting the ground state with vibrational states higher than the first and these are inaccessible, relative to the first vibrational state, at thermal energies. We assume that the only part of the intermolecular force which gives rise to vibrational transitions is the component along the internuclear axis. This is

$$\text{B.35)} \quad \vec{F} \cdot \hat{\xi}_1 = - \frac{\partial V}{\partial R} \hat{R} \cdot \hat{\xi}_1 = \frac{2V'_O}{L} \frac{m_1 - m_2}{m_{12}} \cos^2 \chi_1 \xi_1 e^{-R/L} .$$

Averaged over orientations of the CO molecule this is

$$\text{B.36)} \quad \int \vec{F} \cdot \hat{\xi}_1 d\Omega = \frac{2}{3} \frac{V'_O}{L} \frac{m_1 - m_2}{m_{12}} \xi_1 e^{-R/L} .$$

The spherically symmetric form of the potential which we may use in the vibrational calculation is thus

$$\text{B.37)} \quad V(R, \xi) = V_O \left(1 + a \frac{\xi}{L} \right) e^{-R/L} ,$$

where

$$\text{B.38) } V_0 = 4V'_0 \quad \text{and} \quad a = \frac{1}{6} \frac{m_1 - m_2}{m_{12}} .$$

We now turn to the problem posed by equation B.18. The first step in obtaining a solution is to make what is known as the distorted wave approximation. In the one-dimensional case this approximation would be sufficient to effect a solution. In addition to off-diagonal matrix elements in B.19 being small relative to diagonal elements, we assume that the amplitudes of inelastically scattered waves are small, and thus that products of small quantities appearing in B.18 may be ignored. The set of equations B.18 may then be written as two coupled equations for the elastically and inelastically scattered waves

$$\text{B.39) } \left[\frac{d^2}{dr^2} - \frac{l(l+1)}{r^2} + k_n^2 - \frac{2\mu}{\hbar^2} \langle n | V | n \rangle \right] u_{nn}^l(r) = 0$$

$$\begin{aligned} \text{B.40) } \left[\frac{d^2}{dr^2} - \frac{l(l+1)}{r^2} + k_{n'}^2 - \frac{2\mu}{\hbar^2} \langle n' | V | n' \rangle \right] u_{nn'}^l(r) \\ = \frac{2\mu}{\hbar^2} \langle n | V | n' \rangle u_{nn}^l(r) \end{aligned}$$

Primed quantities refer to the inelastically scattered wave. Denote by $w_{nn}^l(r)$ and $w_{nn'}^l(r)$ the solutions of B.39 and of the homogeneous equation corresponding to B.40, respec-

tively, which have the asymptotic behavior

$$B.41) \quad w_{nn'}^l(r) \approx \sin(k_n r - \frac{l\pi}{2} + \eta_{nn'}^l) ,$$

and let $\mathcal{J}_{nn'}^l(r)$ be the solutions of these equations which behave asymptotically as

$$B.42) \quad \mathcal{J}_{nn'}^l(r) = \frac{1}{k_n} e^{i(k_n r - \frac{l\pi}{2} + \eta_{nn'}^l)} .$$

Then the solution of the inhomogeneous equation B.40 is, from Mott and Massey (1965),

$$B.43) \quad u_{nn'}^l(r) = \delta_{nn'} w_{nn'}^l(r) + (1 - \delta_{nn'}) \frac{2\mu}{\hbar^2} \\ \times \left[\mathcal{J}_{nn'}^l \int_0^r w_{nn'}^l \langle n|V|n' \rangle w_{nn'}^l dr \right. \\ \left. + w_{nn'}^l \int_r^\infty \mathcal{J}_{nn'}^l \langle n|V|n' \rangle \mathcal{J}_{nn'}^l dr \right] ,$$

which behaves asymptotically as

$$B.44) \quad u_{nn'}^l(r) \approx \delta_{nn'} \sin(k_n r - \frac{l\pi}{2} + \eta_{nn'}^l) \\ + (1 - \delta_{nn'}) e^{i(k_n r - \frac{l\pi}{2} + \eta_{nn'}^l)} \beta_{nn'}^l ,$$

where

$$\text{B.45)} \quad \beta_{nn'}^l = \frac{2\mu}{\hbar^2 k_{n'}} \int_0^\infty \omega_{nn'}^l \langle n | V | n' \rangle \omega_{nn'}^l dr \quad .$$

We recall that the scattering matrix was defined in terms of the asymptotic behavior of $u_{nn'}^l$, (B.11). Comparing B.11 and B.43, we find that the scattering matrix, in the distorted wave approximation, is given by

$$\text{B.46)} \quad S^l(n, n') = e^{i(\eta_{nn'}^l + \eta_{nn'}^l)} \left[\frac{k_{n'}}{k_n} \right]^{\frac{1}{2}} \left[\delta_{nn'} (1 - 2i\beta_{nn'}^l) + 2i\beta_{nn'}^l \right] \quad .$$

Substituting B.46 into B.17, using B.14, results in the following total collisional cross section

$$\text{B.47)} \quad \sigma(n, n') = 4\pi \frac{k_{n'}}{k_n^3} \sum_{l=0}^{\infty} (2l+1) \left| \beta_{nn'}^l \right|^2 \quad .$$

To evaluate $\beta_{nn'}^l$, from B.45, the differential equation B.39 for the function $\omega_{nn'}^l(r)$ must first be solved. As it stands, B.39 cannot be integrated in terms of known functions. Integration is possible, however, if a further approximation, known as the method of modified wave number (Takayanagi, 1954), is made. We observe that the centrifugal potential $l(l+1)/r^2$ varies slowly compared with the repulsive part of the intermolecular potential, and will therefore assume that

the only effect of the long-range forces, centrifugal as well as attractive, is to shift the effective collision velocity from w_o to w , where

$$B.48) \quad w^2 = w_o^2 - \left[\frac{\hbar^2}{2\mu} \right] \frac{\ell(\ell+1)}{r_c^2} + \frac{2\epsilon}{\mu} \quad .$$

The effect of the van der Waals forces has already been absorbed in the wave number k since the potential was given the form B.30. The same is now done with the centrifugal potential, and B.37 is written

$$B.49) \quad \left[\frac{d^2}{dr^2} + k^2 - \frac{2\mu}{\hbar^2} V_o e^{-r/L} \right] w_{nn'}^{\ell}(r) = 0 \quad ,$$

where B.35 for $V(R, \xi)$ has been used along with orthonormality of the oscillator eigenfunctions. Changing the independent variable in B.47 to

$$B.50) \quad y = 2L \sqrt{\frac{2\mu V_o}{\hbar^2}} e^{-r/2L}$$

B.49 becomes

$$B.51) \quad \frac{d^2 w_{nn'}^{\ell}}{dy^2} + \frac{1}{y} \frac{dw_{nn'}^{\ell}}{dy} + \left[\frac{q'^2}{y^2} - 1 \right] w_{nn'}^{\ell} = 0 \quad ,$$

where $q' = 2Lk_{n'}$. This is Bessel's equation of imaginary

argument iy and imaginary index iq' , and its solution has been presented by Jackson and Mott (1932). The solution which satisfies the boundary conditions

$$\omega_{nn'}^l(r) \approx \sin(k_{n'}r + \eta_{nn'}^l) \quad \text{as } y \rightarrow 0$$

B.52)

$$\omega_{nn'}^l(r) \approx 0 \quad \text{as } y \rightarrow \infty$$

may be written

$$\text{B.53)} \quad \omega_{nn'}^l(y) = \left[\frac{q' \sinh \pi q'}{\pi} \right]^{\frac{1}{2}} K_{iq'}(y) \quad .$$

With this solution of the Schrodinger equation, the factor $|\beta_{nn'}^l|^2$ in B.47 can be evaluated. The l -dependence of this term is implicit in the wave number. Using B.37 for $V(R, \xi)$ and B.43 for $\beta_{nn'}^l$, we have

$$\text{B.54)} \quad \beta_{nn'}^l = \frac{2\mu V_0}{\hbar^2 k_{n'}} \frac{H_{01}}{L} a \int_0^\infty \omega_{nn'}^l(r) \omega_{nn'}^l(r) e^{-r/L} dr \quad ,$$

and with the variable transformation given by B.50, this is

$$\text{B.55)} \quad \beta_{nn'}^l = \frac{a}{2\pi^2} \frac{H_{01}}{k_{n'} L} \left[gg' \sinh g \sinh g' \right]^{\frac{1}{2}} \\ \times \int_0^Y K_{iq}(y) K_{iq'}(y) y dy \quad ,$$

where $g = \pi q$ and $y_0 = 2L\sqrt{(2\mu V_0)/\hbar^2}$. In terms of quantities $\theta = \hbar v/\kappa$ and $\theta' = \epsilon'/\kappa$, the upper limit of this integral may be written

$$\text{B.56)} \quad y_0 = \frac{1}{\pi\theta} \sqrt{2\theta' \frac{V_0}{\kappa}},$$

where κ is Boltzmann's constant. V_0 is determined from

$$\text{B.57)} \quad V_0 e^{-r_c/L} = E_m + \epsilon$$

or

$$\text{B.58)} \quad \frac{V_0}{\kappa} e^{-r_c/L} = \frac{1}{2} \left[\frac{\theta}{T} \right]^{1/3} T + \frac{\epsilon}{\kappa}.$$

Herzfeld and Litovitz (1959) give $\epsilon/\kappa \approx 100^\circ\text{K}$ and, typically $\theta \geq 1000^\circ\text{K}$. Hence, the second term on the right hand side of B.58 may be neglected and

$$\text{B.59)} \quad y_0 = \frac{1}{\pi} \frac{T}{\theta} \left[\frac{\theta'}{T} \right]^{2/3} e^{r_c/2L}.$$

For various collision processes the factor in front of the exponential varies from about 3 to 60 and $8 < r_c/2L < 11$; hence, the upper limit y_0 in B.55 may, without risk of appreciable error, be replaced by ∞ . With this done the

integral may be evaluated with the result

$$\text{B.60)} \quad \beta_{nn'}^{\ell} = \frac{a}{8\pi^2} \frac{|H_{01}|}{L^2 k_{n'}} \sqrt{gg'} (g'^2 - g^2) \frac{(\sinh g' \sinh g)^{\frac{1}{2}}}{\cosh g' - \cosh g} .$$

$g = 2\pi L/\lambda$ where λ is the DeBroglie wavelength. At thermal energies for an H_2 molecule $\lambda \approx .175\text{\AA}$ and is shorter for heavier particles. Generally, $L \approx 0.2\text{\AA}$, hence, $g \gtrsim 7$ and $\sinh g \approx \cosh g \approx \frac{1}{2}e^g$. With this approximation the square of B.60 becomes

$$\text{B.61)} \quad |\beta_{nn'}^{\ell}|^2 = \left[\frac{a}{8\pi^2} \right]^2 \frac{|H_{01}|^2}{(L^2 k_{n'})^2} gg' (g'^2 - g^2)^2 \frac{e^{g-g'}}{(1 - e^{g-g'})^2} .$$

This expression is independent of the sign of $g - g'$. We will assume that $g - g'$ as well as g and g' is much greater than one. This assumption restricts the validity of what follows to collisions in which a large change in translational energy occurs. With this assumption we have

$$\text{B.62)} \quad |\beta_{nn'}^{\ell}|^2 = \left[\frac{a}{8\pi^2} \right]^2 \frac{|H_{01}|^2}{(L^2 k_{n'})^2} gg' (g'^2 - g^2)^2 e^{-|g-g'|} .$$

We will write the cross section of B.47 as

$$\text{B.63)} \quad \sigma(n, n') = \sum_{\ell} (2\ell+1) \sigma_{nn'}^{\ell} ,$$

where $\sigma_{nn'}^{\ell}$ is defined as

$$\text{B.64)} \quad \sigma_{nn'}^{\ell} = 4\pi \frac{k_{n'}}{k_n^3} \left| \beta_{nn'}^{\ell} \right|^2 .$$

Using B.62 this is

$$\text{B.65)} \quad \sigma_{nn'}^{\ell} = \frac{a^2}{16\pi^3} \frac{|H_{01}|^2}{L^4} \frac{1}{k_n^3 k_{n'}^3} g g' (g'^2 - g^2)^2 e^{-|g-g'|} .$$

It must be recalled that the ℓ -dependence on the right hand side is implicit in the wave number, which means it is also contained in the factors g and g' . We can write out this dependence in explicit form as

$$\begin{aligned} \text{B.66)} \quad k'^2 &= k_1^2 + \frac{2\mu\epsilon}{\hbar^2} - \frac{\ell(\ell+1)}{4r_c^2} \\ k^2 &= k_0^2 + \frac{2\mu\epsilon}{\hbar^2} - \frac{\ell(\ell+1)}{4r_c^2} , \end{aligned}$$

where k_1 and k_0 are the wave numbers which would pertain in the absence of long-range forces. Using B.66 we have

$$\text{B.67)} \quad g'^2 - g^2 = g_1^2 - g_0^2 = \left[\frac{2\pi L}{\hbar} \right]^2 (p_1^2 - p_0^2) = - \left[\frac{2\pi L}{\hbar} \right]^2 2\mu h\nu .$$

Also $g g' / k k' = 4\pi^2 L^2$. At this point the cross section is

$$\text{B.68)} \quad \sigma_{nn'}^{\ell} = \frac{a^2}{\pi} \frac{|H_{01}|^2}{L^2} \frac{1}{k_n^2} \left[\frac{\epsilon'}{h\nu} \right]^2 e^{-|g-g'|} ,$$

where B.21, defining ϵ' , has been used. To express the cross section as a function of molecular speed, we write

$$|g - g'| = \frac{2\pi L}{h} |p - p'|, \text{ and with } p'^2 = p^2 - 2\mu h\nu$$

$$\text{B.69)} \quad |p - p'| = p \left[1 - \sqrt{1 - \frac{2\mu h\nu}{p^2}} \right] = \frac{h\nu}{w} \left[1 + \frac{h\nu}{2\mu w^2} \right].$$

As a function of w then

$$\text{B.70)} \quad \sigma_{nn'}^{\ell} = \frac{a^2}{\pi} \left[\frac{h}{\mu} \right]^2 \frac{|H_{01}|^2}{L^2} \left[\frac{\epsilon'}{h\nu} \right]^2 \frac{1}{w^2} e^{-\frac{4\pi^2 L\nu}{w} \left[1 + \frac{h\nu}{2\mu w^2} \right]}.$$

The long-range forces, van der Waals and centrifugal, are still contained implicitly in w . These may be taken into account after $\sigma_{nn'}^{\ell}$ is averaged over the Maxwellian velocity distribution.

The integral which must be evaluated is

$$\text{B.71)} \quad I = 4\pi \left[\frac{\mu}{2\pi kT} \right]^{3/2} \int_0^{\infty} w e^{-\left[\frac{\mu w^2}{2kT} + \frac{4\pi^2 L\nu}{w} \left(1 + \frac{h\nu}{2\mu w^2} \right) \right]} dw.$$

As a first step in obtaining an approximate evaluation of this integral, Herzfeld and Litovitz (1959) divide the integrand into two factors, i.e., they write the integrand as

$$\text{B.72)} \quad f(w) e^{-\left[\frac{\mu w^2}{2kT} + \frac{4\pi^2 L\nu}{w} \right]}.$$

The exponential factor is sharply peaked at some velocity w_m and the argument of the exponential may be expanded about this velocity. The factor $f(w)$ is evaluated at $w = w_m$ and removed from the integral sign. Denoting the argument of the exponential by $g(w)$ we write

$$\text{B.73)} \quad g(w) = g(w_m) + g'(w_m)(w-w_m) + \frac{1}{2}g''(w_m)(w-w_m)^2 + \dots$$

the primes denoting differentiation and

$$g(w) = \frac{\mu w^2}{2\kappa T} + \frac{4\pi^2 L_V}{w}$$

$$\text{B.74)} \quad g'(w) = \frac{\mu w}{\kappa T} - \frac{4\pi^2 L_V}{w^2}$$

$$g''(w) = \frac{\mu}{\kappa T} + \frac{8\pi^2 L_V}{w^3} \quad .$$

Setting $g'(w) = 0$ we find that the exponential is peaked about the velocity

$$\text{B.75)} \quad w_m = \left[\frac{4\pi^2 L_V \kappa T}{\mu} \right]^{1/3} \quad .$$

Using B.75 along with B.22 we have

$$\text{B.76)} \quad e^{-g(w)} = e^{-\frac{3}{2} \left[\frac{\epsilon'}{\kappa T} \right]^{1/3}} e^{-\frac{3}{2} \frac{\mu}{\kappa T} (w-w_m)^2} \quad .$$

The integral B.71 may now be evaluated with the result that

$$\text{B.77) } \langle \sigma_{nn,w}^{\ell} \rangle = \frac{a^2}{\sqrt{3} \pi} \left[\frac{\hbar}{\mu} \right]^2 \left[\frac{\epsilon'}{\hbar v} \right]^2 \left[\frac{\epsilon'}{\kappa T} \right]^{1/6} \left[\frac{\mu}{\kappa T} \right]^{1/2} \frac{|H_{01}|^2}{L^2} \\ \times e^{-\frac{3}{2} \left[\frac{\epsilon'}{\kappa T} \right]^{1/3} - \frac{\hbar v}{2\kappa T}}.$$

The existence of long-range forces has not yet been taken into account. We may assume that Maxwell's distribution law is valid, but that the long-range forces have the effect of changing the local density of colliding molecules by a factor $e^{(\epsilon - \epsilon_{\ell})/\kappa T}$, where $\epsilon_{\ell} = \frac{\hbar^2}{2\mu} \frac{\ell(\ell+1)}{r_c^2}$. The averaged cross section in B.77 should therefore also be changed by this factor, and we have

$$\text{B.78) } \langle \sigma_{nn,w}^{\ell} \rangle = \frac{a^2}{\sqrt{3} \pi} \left[\frac{\hbar}{\mu} \right]^2 \left[\frac{\epsilon'}{\hbar v} \right]^2 \left[\frac{\epsilon'}{\kappa T} \right]^{1/6} \left[\frac{\mu}{\kappa T} \right]^{1/2} \frac{|H_{01}|^2}{L^2} \\ \times e^{-\frac{3}{2} \left[\frac{\epsilon'}{\kappa T} \right]^{1/2} - \frac{\hbar v}{2\kappa T} + \frac{(\epsilon - \epsilon_{\ell})}{\kappa T}}.$$

B.78 must still be summed over ℓ according to B.63 before the final expression for $\eta(T)$ can be written. The only ℓ -dependence on the right hand side of B.78 is in the term $e^{-\epsilon_{\ell}/\kappa T}$, and the sum to be calculated is just $\sum_{\ell} (2\ell+1) e^{-\epsilon_{\ell}/\kappa T}$. If the angular momentum levels are close

in energy, relative to the thermal energy, the sum may be replaced by the integral

$$\text{B.79)} \quad \sum_{\ell} (2\ell+1) e^{-\epsilon_{\ell}/\kappa T} \rightarrow \frac{2\mu r_c^2}{h^2} \int_0^{\infty} e^{-\epsilon/\kappa T} d\epsilon_{\ell} = \frac{2\mu r_c^2}{h^2} \kappa T \quad .$$

With this assumption the expression for $\eta(T)$ is finally

$$\text{B.80)} \quad \eta(T) = \frac{2a^2}{\sqrt{3} \pi} \left[\frac{\epsilon'}{\kappa T} \right]^{1/6} \left[\frac{\kappa T}{\mu} \right]^{1/2} \frac{|H_{01}|^2}{L^2} r_c^2 e^{-\frac{3}{2} \left[\frac{\epsilon'}{\kappa T} \right]^{1/3} - \frac{h\nu}{2\kappa T} + \frac{\epsilon'}{\kappa T}} \quad .$$

With the values $\epsilon'/\kappa = 1.08$, $|H_{01}|^2/L^2 = 1.19 \times 10^{-2}$,
 $\epsilon/\kappa = 100^\circ\text{K}$, $r_c = 3.69 \times 10^{-8}$ as given by Herzfeld and
 Litovitz (1959), and using μ appropriate to a CO-N₂ system,
 we have

$$\text{B.81)} \quad \eta_{\text{CO}}(T) = 2.4 \times 10^{-17} T^{1/3} e^{-\frac{195}{T^{1/3}} - \frac{1500}{T}} \quad .$$

This activation coefficient is so small that radiative cooling from vibrational states of CO will be negligible.

ACKNOWLEDGEMENTS

This research was conducted at the Goddard Institute for Space Studies of the National Aeronautics and Space Administration under the supervision of Dr. Robert Jastrow. Dr. Jastrow originally suggested this area of research and I am grateful for his support. This paper owes much to his helpful discussion of many of the topics involved.

I am grateful to Dr. I. Rasool for his interest and advice on several points pertinent to this work and to Dr. M. J. McElroy for reading the manuscript and offering constructive criticisms.

The staff of Computer Applications, Inc. was very helpful in elucidating some of the problems involved in programming the calculations, in overcoming the problems attendant to the operation of a new computing facility, and in distinguishing between the two. I especially thank Conrad Hipkins and John Borgelt for their assistance.

This research was supported in part by the National Aeronautics and Space Administration under Grant Number NSG-445 to Columbia University.

REFERENCES

- Arthurs, A. M., and A. Dalgarno, Proc. Roy. Soc. London A256, 540 (1960).
- Barth, C. A., Ann. Geophys. 20, 182 (1964).
- Bates, D. R., Proc. Phys. Soc. London B64, 805 (1951).
- Biondi, M. A., Ann. Geophys. 20, 34 (1964).
- Blatt, J. M., and L. C. Biedenharn, Rev. Mod. Phys. 24, 258 (1952).
- Brace, L. H., Spencer, N. W., and G. R. Carignan, J. Geophys. Res. 68, 5397 (1963).
- Chamberlain, J. W., Ap. J. 136, 582 (1962).
- Chamberlain, J. W., and M. B. McElroy, Science 152, 21 (1966).
- Chapman, S., and T. G. Cowling, The Mathematical Theory of Non-uniform Gases, 2d ed. (Cambridge Univ. Press, Cambridge, 1952).
- Dalgarno, A., McElroy, M. B., and R. J. Moffett, Planet. Space Sci. 11, 463 (1963).
- Dalgarno, A., and D. Parkinson, J. Atmospheric Terrest. Phys. 18, 335 (1960).
- Davison, W. D., Disc. Faraday Soc. 33, 71 (1961).
- DeWette, F. W., and Z. I. Slawsky, Physica 20, 1169 (1954).
- Fano, U., and G. Racah, Irreducible Tensorial Sets (Academic Press, New York, 1959).
- Fjeldbo, G., Fjeldbo, W. C., and V. R. Eshleman, J. Geophys. Res. 71, 2307 (1966a).
- Fjeldbo, G., Fjeldbo, W. C., and V. R. Eshleman, Science 153, 1518 (1966b).

- Fowler, R. H., Statistical Mechanics, 2d ed. (Cambridge Univ. Press, Cambridge, 1955).
- Goody, R. M., Atmospheric Radiation: I. Theoretical Basis (Clarendon Press, Oxford, 1964).
- Harris, I., and W. Priester, J. Atmospheric Sci. 19, 286 (1962).
- Harteck, P., Reeves, R. R. Jr., Thompson, B. A., and R. W. Waldron, Tellus 18, 192 (1966).
- Herzfeld, K. F., and T. A. Litovitz, Absorption and Dispersion of Ultrasonic Waves (Academic Press, New York, 1959).
- Hinteregger, H. E., Hall, L. A., and G. Schmidtke, in Space Research V, ed. P. Muller (North-Holland Publishing Co., Amsterdam, 1965), p. 1175.
- Hirschfelder, J. O., Curtiss, C. F., and R. B. Bird, Molecular Theory of Gases and Liquids (Wiley, New York, 1954).
- Hunt, D. C., and T. E. van Zandt, J. Geophys. Res. 66, 1673 (1961).
- Jackson, J. M., and N. F. Mott, Proc. Roy. Soc. London A137, 703 (1932).
- Jastrow, R., and L. Kyle, in Handbook of Astronautical Engineering, ed. H. H. Koelle (McGraw-Hill, New York, 1961), p. 2.
- Johnson, F. S., Science 150, 1445 (1965).
- Kaplan, L. D., Munch, G., and H. Spinrad, Ap. J. 139, 1 (1964).
- Kliore, A., Cain, D. L., Levy, G. S., Eshleman, V. R., Fjeldbo, G., and F. D. Drake, Science 149, 1243 (1965).
- Kuo, S. S., Numerical Methods and Computers (Addison-Wesley, Reading, Mass., 1965).

- Lazarev, V. I., Geomagn. i. Aeronomiya 3, 842 (1963); NASA Draft Translation ST-AI-10094 (1964).
- McElroy, M. B., L'Ecuyer, J., and J. W. Chamberlain, Ap. J. 141, 1523 (1965).
- Mange, P., J. Geophys. Res. 62, 279 (1957).
- Marmo, F. F., and P. Warneck, in Planetary Atmosphere Studies VIII, GCA Technical Report 61-20-N (1961).
- Mott, N. F., and H. S. W. Massey, The Theory of Atomic Collisions, 3d ed. (Clarendon Press, Oxford, 1965).
- Nicolet, M., J. Atmospheric Terrest. Phys. 5, 132 (1954).
- Nicolet, M., in Physics of the Upper Atmosphere, ed. J. A. Ratcliffe (Academic Press, New York, 1960), p. 17.
- Nicolet, M., and P. Mange, J. Geophys. Res. 59, 15 (1954).
- Norton, R. B., Ferguson, E. E., Feshenfeld, F. C., and A. L. Schmeltekopf, Planet. Space Sci. 14, 969 (1966).
- Owen, T., Ap. J. 146, 257 (1966).
- Priester, W., Proc. Roy. Soc. London A288, 493 (1965).
- Sagalyn, R. C., M. Smiddy, and Y. N. Bhargava, in Space Research V, ed. P. Muller (North-Holland Publishing Co., Amsterdam, 1965), p. 189.
- Schiff, L. I., Quantum Mechanics, 2d ed. (McGraw-Hill, New York, 1955).
- Schwartz, R. N., and K. F. Herzfeld, J. Chem. Phys. 22, 767 (1954).
- Schwartz, R. N., Slawsky, Z. I., and K. F. Herzfeld, J. Chem. Phys. 20, 1591 (1952).
- Shimizu, M., Planet. Space Sci. 11, 269 (1963).
- Schultz, E. D., and A. C. Holland, NASA Contractor Report CR-11 (1963).

Schultz, E. D., Holland, A. C., and F. F. Marmo, NASA Contractor Report CR-15 (1963).

Spencer, N. W., Brack, L. H., Carignan, G. R., Taeusch, D. R., and H. N. Niemann, J. Geophys. Res. 70, 2665 (1965).

Spinrad, H., Schorn, R. A., Moore, R., Giver, L. P., and H. J. Smith, Ap. J. 146, 331 (1966).

Sutton, W. G. L., Proc. Roy. Soc. London A182, 48 (1943).

Takayanagi, K., Progr. Theor. Phys. Japan 8, 497 (1952).

Takayanagi, K., Progr. Theor. Phys. Japan 11, 557 (1954).

Walker, J. C. G., The Day Airglow and the Heating of the Upper Atmosphere, unpublished Ph.D. dissertation, Columbia University (1964).

Watson, G. N., A Treatise on the Theory of Bessel Functions, 2d ed. (Cambridge Univ. Press, Cambridge, 1944).

Wray, K. L., AVCO Research Rept. 104 (1961).

Yonezawa, T., Space Sci. Rev. 5, 3 (1965).

Zener, C., Phys. Rev. 37, 556 (1931).